AD-A114 460 NOTRE DAME UNIV IN DEPT OF CIVIL ENGINEERING F/G 9/2
A VISCOPLASTIC ALGORITHM FOR CAP75.(U)
MAY 82 M G KATONA, M A MULERT N68305-80-C-0031
UNCLASSIFIED CEL-CR-82.021 NL

END
DATE FILMED
6 82
DTIC

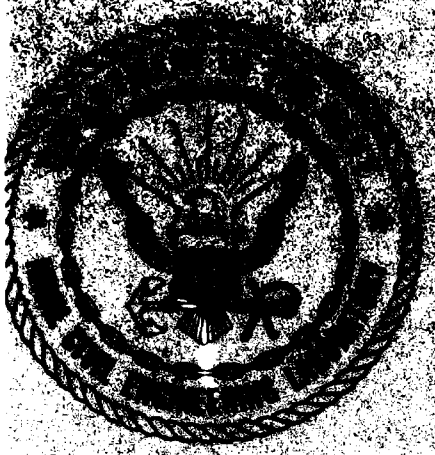

Naval Civil Engineering Laboratory
Port Hueneme, California

Sponsored by
NAVAL FACILITIES ENGINEERING COMMAND

A VISCOPLASTIC ALGORITHM FOR CAP75

May 1982

An Investigation Conducted by
DEPARTMENT OF CIVIL ENGINEERING
University of Notre Dame
Notre Dame, Indiana

N62583-80-C-0031

Unclassified

SECURITY CLASSIFICATION OF THIS PAGE (When Data Entered)

REPORT DOCUMENTATION PAGE		READ INSTRUCTIONS BEFORE COMPLETING FORM
1 REPORT NUMBER CR 82.021	2 GOVT ACCESSION NO. AD-A114 460	3 RECIPIENT'S CATALOG NUMBER
4 TITLE (and Subtitle) A Viscoplastic Algorithm for CAP75		5 TYPE OF REPORT & PERIOD COVERED Final Sep 1980 - Sep 1981 6 PERFORMING ORG. REPORT NUMBER
7 AUTHOR(s) Michael G. Katona Mark A. Mulert		8 CONTRACT OR GRANT NUMBER(s) N68305-80-C-0031
9 PERFORMING ORGANIZATION NAME AND ADDRESS Department of Civil Engineering University of Notre Dame Notre Dame, IN 46556		10 PROGRAM ELEMENT, PROJECT, TASK AREA & WORK UNIT NUMBERS 61152N, R000, ZR023-03 ZR-000-01-180
11 CONTROLLING OFFICE NAME AND ADDRESS Naval Civil Engineering Laboratory Port Hueneme, CA 93043		12 REPORT DATE May 1982 13 NUMBER OF PAGES 66
14 MONITORING AGENCY NAME & ADDRESS(if different from Controlling Office)		15 SECURITY CLASS (of this report) Unclassified 15a DECLASSIFICATION DOWNGRADING SCHEDULE

16 DISTRIBUTION STATEMENT (of this Report)

Approved for public release; distribution unlimited

17 DISTRIBUTION STATEMENT (of the abstract entered in Block 20, if different from Report)

18 SUPPLEMENTARY NOTES

19 KEY WORDS (Continue on reverse side if necessary and identify by block number)

Elasticity, plasticity, viscoplasticity, CAP75, model, computer program, Crank-Nicolson, geological, explicit, implicit, strain rate, dynamic yield strength

20 ABSTRACT (Continue on reverse side if necessary and identify by block number)

A viscoplastic formulation based on Perzyna's elastic/viscoplastic theory is developed for geological materials using the Sandler and Rubin CAP75 plasticity model. The numerical strategy employs a one parameter Crank-Nicolson time integration scheme which provides options for explicit and implicit algorithms. A computer program called VPDRVR exercises these algorithms for arbitrary states of stress or strain.

DD FORM 1 JAN 73 1473 EDITION OF 1 NOV 65 IS OBSOLETE

Unclassified

SECURITY CLASSIFICATION OF THIS PAGE (When Data Entered)

A VISCOPLASTIC ALGORITHM FOR CAP75

CONTENTS

INTRODUCTION

Objective. The specific objective is to formulate a viscoplastic constitutive model which incorporates the so-called "CAP75" plasticity model for geological materials (1). Included in this objective is the development of a numerical solution algorithm (computer program) which "exercises" the viscoplastic model for general states of strain loading (or stress loading) time histories.

Background. Geological constitutive models based on inviscid plasticity concepts, such as CAP75, are inherently independent of real time. Experimental evidence, however, indicates a strong time-dependent behavior for most soils and rocks (2,3,4,5), thus motivating the above objective. The coupling of plastic behavior with time dependency comes under the general heading of viscoplasticity. Like religion, viscoplasticity has a variety of "sects" each with its own fervent disciples, dogmas, claims and counterclaims. Some perspective on the variety of viscoplastic formulations can be gained by contrasting the endochronic approach of Valinis (6) to the elastic/viscoplastic approach of Perzyna (7). The genesis of the former may be envisioned as a modification to classical viscoelasticity wherein plastic-like behavior is introduced by means of "intrinsic time", a time scale considered to be a property of the material. No plastic yield function is introduced. Alternatively, Perzyna's elastic/viscoplastic approach is a modification of classical plasticity wherein viscous-like behavior is introduced by a time rate flow rule which employs a plastic yield function. Other viscoplastic formulations include developments by Katona (8), Bodner and Parton (9), and Phillips and Wu (10).

Any viscoplastic formulation should have the following attributes: (1) capability of simulating observed material behavior over a wide range of loading conditions; (2) satisfaction of thermodynamic restrictions; (3) feasible techniques for parameter identification; and (4) readily adaptable and efficient in numerical solution procedure (e.g. finite element methods). With regard to the last attribute, the numerical solution strategy is clearly of utmost importance, i.e. it makes no sense to utilize sophisticated constitutive theories if the accuracy of the solution is highly questionable. At the same time, however, some compromise in accuracy must be made to achieve computational efficiency.

In 1974 Zienkiewicz and Cormeau (11) presented a finite element algorithm for a viscoplastic model of the Perzyna type using an explicit forward difference scheme for time integration. Computationally the explicit algorithm is simple, requiring only an elastic stiffness matrix to be assembled and triangularized at the outset. Nonlinearities are accomodated on the right-hand-side at the element level with (if desired) a mid-interval iteration and/or next-interval equilibrium correction (12). Unfortunately, a major drawback is the concern for numerical stability. This places a stringent limit on the size of the time step and, thereby, compromises overall efficiency. Cormeau (13) presented a priori time step limits to avoid instability for a restricted class of Perzyna-type viscoplastic models. However, for more general forms (e.g. viscoplastic models with hardening) a priori time step limits are not established.

Numerical stability concerns can be eliminated by employing an implicit time integration scheme. Hughes and Taylor (14) showed that a one parameter (θ) Crank-Nicolson integration scheme provides unconditional stability for $0.5 \leq \theta \leq 1$ when applied to FEM models with Perzyna-type viscoplasticity. For a particular problem, they demonstrated accuracy was maintained for implicit time-step sizes 10^5 times greater than the critical time-step size in the explicit algorithm.

The computational penalty for implicit integration schemes is the requirement to solve nonlinear algebraic equations for each time step. Here a variety of efficiency vs. accuracy alternatives are possible based on various versions of the Newton-Raphson technique (15,16).

Scope and Approach. In meeting the stated objective, a Perzyna-type viscoplastic formulation is adopted. Motivations for this choice are; (1) the formulation is well accepted and well used, and (2) the incorporation of the CAP75 plasticity model (or any plasticity model) is theoretically straightforward. In contrast, the endochronic approach to viscoplasticity continues to draw criticism and does not lend itself to direct incorporation of plasticity models.

For this study, a one parameter Crank-Nicolson time integration scheme is used which provides options for explicit or implicit algorithms. For the implicit algorithm, nonlinear algebraic equations are solved "exact-as-desired" by an iterative Newton-Raphson technique with special modifications for plastic hardening.

For clarity and insight, the presentation begins with a one-dimensional viscoplastic formulation along with some exact solutions illustrating the influence of viscoplastic model parameters. The numerical time integration is also introduced at the one-dimensional level illustrating the nature of explicit and implicit algorithms. Next, the general multi-dimensional viscoplastic formulation is presented together with the numerical solution strategy. Finally, the formulation is specialized for the CAP75 plasticity model and example results are discussed.

The Appendix contains user input instructions for the computer program VPDRVR which is a viscoplastic version of the plasticity program CAPDRVR (17).

ONE-DIMENSIONAL VISCOPLASTICITY

Although one dimensional viscoplastic stress-strain relationships have limited practical application, they provide an excellent starting point for introducing fundamental theoretical concepts, behavior characteristics, and solution strategies.

Conceptual Formulation. Figure 1 illustrates a simple viscoplastic rheological model composed of an elastic element (e.g. spring), viscous element (e.g. dashpot), and a plastic element (e.g. slider). In such a rheological construction we first identify local stress-strain relations of the component elements. As a somewhat general example, we will specify the following forms.

For the elastic element let:

$$\sigma_e = E(\varepsilon_e) \tag{1}$$

where σ_e, ε_e = stress and strain in elastic element

$E(\varepsilon_e)$ = modulus function of elastic strain, (linear case $E(\varepsilon_e) = E_0\varepsilon_e$).

In Equation (1), the inverse is required to exist, i.e., $\varepsilon_e = E^{-1}(\sigma_e)$.

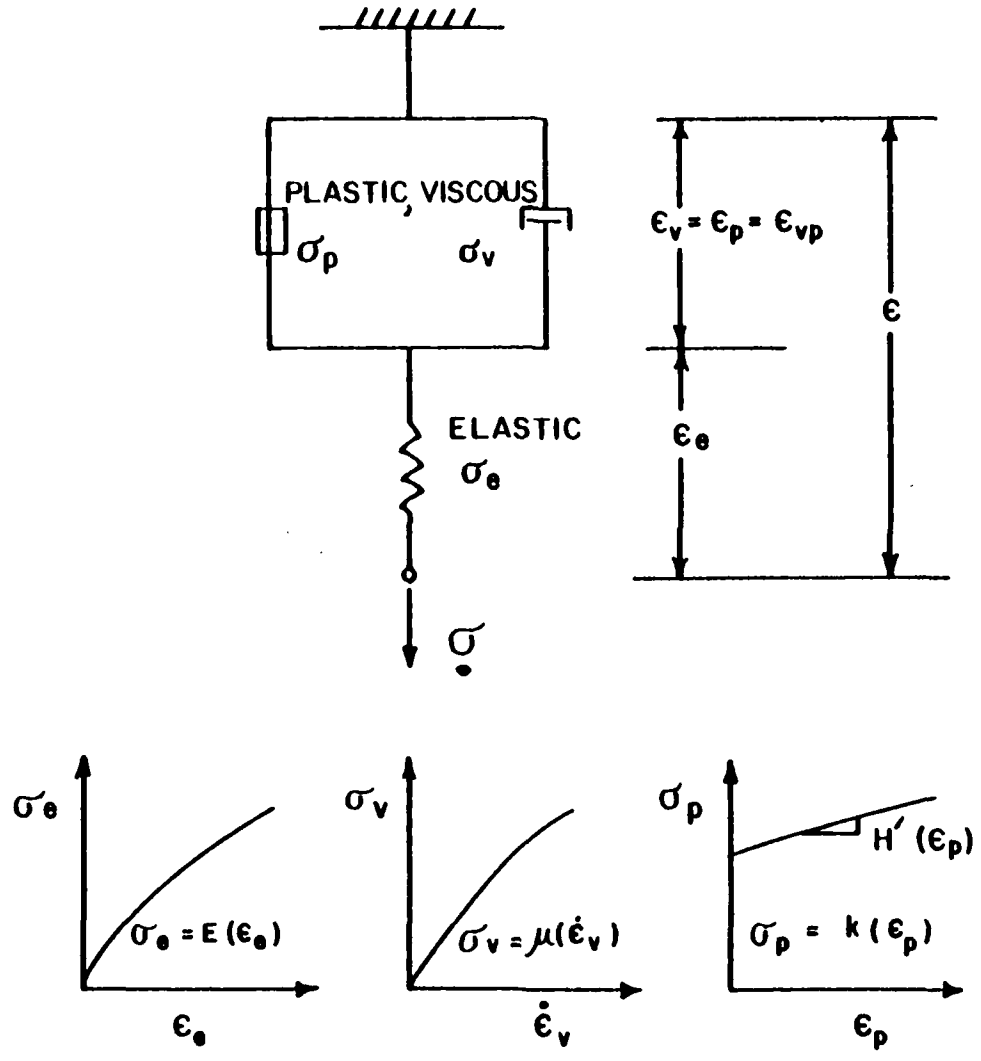

Figure 1. One dimensional viscoplastic model.

The viscous stress-strain relation is represented in power form as:

$$\dot{\varepsilon}_v = \gamma \left(\frac{|\sigma_v|}{\sigma_0} \right)^N \text{sgn } (\sigma_v) \qquad (2)$$

where $\dot{\varepsilon}_v$ = rate of viscous straining, $d\varepsilon_v/dt$.

σ_v = viscous stress.

σ_0 = normalizing constant (units of stress).

γ = fluidity parameter (units of inverse time).

N = exponent power ($N > 0$).

$$\text{sgn } (\sigma_v) = \begin{cases} +1, & \sigma_v > 0 \\ -1, & \sigma_v < 0 \end{cases}$$

Note the linear form of Equation 2 is given by $N = 1$ representing a simple dashpot model. In such a case the dashpot coefficient is $\mu = \sigma_0/\gamma$, (i.e. $\dot{\varepsilon}_v = \sigma_v/\mu$). In the more general case ($N \neq 1$) Equation 2 is a nonlinear creep law implying that the viscous strain rate magnitude is proportional to some power of the viscous stress, and the strain rate direction (sign) is governed by the viscous stress sign.

Lastly, the plastic element is defined by means of an isotropic hardening plastic yield function f;

$$f(\sigma_p, \varepsilon_p) = |\sigma_p| - k(\varepsilon_p) \leq 0 \qquad (3)$$

where σ_p, ε_p = stress and strain in plastic element.

$k(\varepsilon_p)$ = positive valued hardening function (for non hardening $k(\varepsilon_p) = k_0$).

In conjunction with the above, we adopt the classical plasticity assumptions that plastic flow (increments of plastic strain) can only occur when the equality holds in Equation 3, i.e.;

$$d\varepsilon_p = \begin{cases} 0, & \text{if } f(\sigma_p, \varepsilon_p) < 0, \\ |d\varepsilon_p| \ \mathrm{sgn}(\sigma_p), & \text{if } f(\sigma_p, \varepsilon_p) = 0, \\ & \text{and } \mathrm{sgn}(\sigma_p) d\sigma_p > 0 \end{cases} \tag{4}$$

Note, $f(\sigma_p, \varepsilon_p) > 0$ is not an admissible state when σ_p is used as an argument in f. This will be elaborated subsequently.

In addition to the above component relationships, the model in Figure 1 inherently implies the following equilibrium and compatability relationships which must always hold true.

$$\sigma = \sigma_e = \sigma_v + \sigma_p \tag{5}$$

$$\varepsilon = \varepsilon_e + \varepsilon_{vp} \tag{6}$$

$$\varepsilon_{vp} = \varepsilon_p = \varepsilon_v \tag{7}$$

$$\mathrm{sgn}(\sigma) = \mathrm{sgn}(\sigma_p) = \mathrm{sgn}(\sigma_v) \tag{8}$$

where σ = total stress

ε = total strain

ε_{vp} = viscoplastic strain

Ultimately the objective is to utilize Equations 1 through 8 to get a differential equation relating total stress to total strain, i.e., a constitutive relation. To this end, Equations 5 and 8 give, $|\sigma_p| = |\sigma| - |\sigma_v|$, which when inserted into Equation 3 with $\varepsilon_p = \varepsilon_{vp}$ allows the left hand side of Equation 3 to be replaced by:

$$f(\sigma_p, \varepsilon_{vp}) = f(\sigma, \varepsilon_{vp}) - |\sigma_v| \tag{9}$$

By virtue of Equation 4 plastic flow occurs when $f(\sigma_p, \varepsilon_{vp}) = 0$ in which case Equation 9 gives $|\sigma_v| = f(\sigma, \varepsilon_{vp})$. Introducing this into Equation 2 with

$\varepsilon_v = \varepsilon_{vp}$, gives;

$$\dot{\varepsilon}_{vp} = \gamma\phi(f)\ \mathrm{sgn}(\sigma) \tag{10}$$

where,
$$\phi(f) = \begin{cases} (f/\sigma_0)^N & \text{when } f > 0 \\ 0 & \text{when } f \leq 0 \end{cases} \tag{11}$$

and, $$f(\sigma, \varepsilon_{vp}) = |\sigma| - k(\varepsilon_{vp}) \tag{12}$$

Equation 10 is a fundamental viscoplastic flow rule of the Perzyna type (7) which could have been simply stated as opposed to the model development given here. However, certain insights from the model development are useful. For example, the so-called "dynamic yield function", given by Equation 12, is greater than zero during plastic flow by the amount $|\sigma_v|$, whereas the classical plasticity yield function is zero during plastic flow (Equation 3). If loading is held constant, steady state conditions are eventually reached, $\sigma_v = \dot{\varepsilon}_{vp} = 0$, so that, $f(\sigma_p, \varepsilon_{vp}) = f(\sigma, \varepsilon_{vp}) = 0$.

To complete the constitutive development Equations 1, 5 and 6 are combined to give:

$$\sigma = E(\varepsilon - \varepsilon_{vp}) \tag{13}$$

Taking the time derivative of Equation 13 and replacing $\dot{\varepsilon}_{vp}$ by Equation 10 gives the final constitutive form:

$$\dot{\sigma} = E(\dot{\varepsilon} - \gamma\phi(f)\ \mathrm{sgn}(\sigma)) \tag{14}$$

In the above, f contains σ and ε_{vp} as an argument, i.e. $f = f(\sigma, \varepsilon_{vp})$, however, we have by Equations 1 and 5:

$$\varepsilon_{vp} = \varepsilon - E^{-1}(\sigma) \tag{15}$$

so that Equation 14 with ε_{vp} given by Equation 15 represents the desired constitutive form relating σ to ε.

Exact Solutions. For present purposes we will consider solutions for Equation 14 as if the model represented a material test specimen with either a specified strain loading history or stress loading history, and we seek the corresponding response history.

To achieve an exact solution we restrict ourselves to linear functional forms for $k(\varepsilon_{vp})$, $\phi(f)$, and $E(\varepsilon_e)$ as follows:

$$k(\varepsilon_{vp}) = \sigma_y + H' \bar{\varepsilon}_{vp} \tag{16}$$

$$\phi(f) = f/\sigma_y, \quad (f > 0) \tag{17}$$

$$E(\varepsilon_e) = E_0 \varepsilon_e \tag{18}$$

with $$f = |\sigma| - (\sigma_y + H' \bar{\varepsilon}_{vp}) \tag{19}$$

and $$\bar{\varepsilon}_{vp} = \int_0^{\varepsilon_{vp}} |d\varepsilon_{vp}| \tag{20}$$

where: E_0 = elastic modulus (positive constant).

σ_y = initial yield stress (positive constant).

H' = plastic hardening modulus (positive constant).

$\bar{\varepsilon}_{vp}$ = viscoplastic strain hardening measure.

Further, if viscoplastic straining is monotonic (i.e., $\dot{\varepsilon}_{vp}$ does not change sign), then $\bar{\varepsilon}_{vp} = |\varepsilon_{vp}|$, or by Equation 15, $\bar{\varepsilon}_{vp} = |\varepsilon - \sigma/E_0|$. Thus, the constitutive relation (Equation 14) becomes the following first order, linear ordinary differential equation when $f > 0$:

$$\dot{\sigma} + \frac{\gamma}{\sigma_y}(E_0 + H')\sigma = E_0(\dot{\varepsilon} + H' \frac{\gamma}{\sigma_y} \varepsilon + \gamma \cdot \mathrm{sgn}(\text{loading})) \tag{21}$$

For the case of stepped strain loading causing viscoplastic flow, we specify:

$$\varepsilon(t) = \beta\varepsilon_y\, h(t) \tag{22}$$

where $\varepsilon_y = \sigma_y/E_0$, initial yield strain (23)

$\beta > 1$, loading magnitude (24)

$$h(t) = \begin{cases} 0 & t < 0^- \\ 1 & t > 0^+ \end{cases} \text{ , heavyside function} \tag{25}$$

The solution to Equation 21 is:

$$\sigma(t) = \sigma_y(\alpha + (\beta - \alpha)\exp(-\gamma(E_0 + H')t/\sigma_y)) \tag{26}$$

where $\alpha = (1 + \beta H'/E_0)/(1 + H'/E_0)$ (27)

consequently, $\beta > \alpha \geq 1$ (28)

Some behaviorial observations from the solution are:

(a) The largest stress occurs instantly at $t = 0^+$, $\sigma(0) = \beta\sigma_y$, which is purely an elastic response, i.e., no time for viscoplastic flow to occur.

(b) The smallest stress occurs when $t \to \infty$, $\sigma(\infty) = \alpha\sigma_y$, which is the elastic-plastic solution, i.e., steady state solution, $\sigma_v = 0$.

(c) The rate of stress decay from $\beta\sigma_y$ to $\alpha\sigma_y$ is controlled by the fluidity parameter, γ. For large values of γ, $\sigma(t)$ approaches $\alpha\sigma_y$ more rapidly. In the limit as $\gamma \to \infty$, $\sigma(t) = \alpha\sigma_y$ for all $t > 0$, inferring the absence of the viscous element.

(d) For nonhardening, $H' = 0$, all the above statements are valid wherein $\alpha = 1$.

The complimentary solution to Equation 21 for a stepped stress loading, defined by;

$$\sigma(t) = \beta\sigma_y h(t) \tag{29}$$

is given by:

$$\varepsilon(t) = \varepsilon_y(\alpha^* - (\alpha^* - \beta)\exp(-\gamma H' t/\sigma_y)) \tag{30}$$

where, $\alpha^* = \frac{E_0}{H'}(\beta - 1) + \beta$ (31)

consequently, $\alpha^* > \beta > 1$ (32)

Some observations from the solution are:

(a) The smallest strain occurs instantly at $t = 0^+$, $\varepsilon(0) = \beta\varepsilon_y$, which is purely an elastic response.

(b) The largest strain occurs when $t \to \infty$, $\varepsilon(\infty) = \alpha^*\varepsilon_y$, which is the steady-state, elastic-plastic solution.

(c) The rate of strain increase from $\beta\varepsilon_y$ to $\alpha^*\varepsilon_y$ occurs more rapidly when the fluidity parameter γ is large.

(d) When the hardening parameter becomes small, $H' \to 0$, we have $\alpha^* \to \infty$ so that $\varepsilon(\infty) \to \infty$ (as expected). In the limit, $H' = 0$, Equation 30 becomes, $\varepsilon(t) = \beta\varepsilon_y + \gamma(\beta - 1)t$.

Numerical Algorithm. Beginning with the rate form of Equation 13,

$$\dot{\sigma} = E(\dot{\varepsilon} - \dot{\varepsilon}_{vp}) \tag{33}$$

we integrate over one time step from time t_n to t_{n+1} to get:

$$\Delta\sigma = E(\Delta\varepsilon - \Delta\varepsilon_{vp}) \tag{34}$$

$$\text{where,} \quad \Delta\sigma = \sigma^{n+1} - \sigma^n = \int_{t_n}^{t_n + \Delta t} \dot{\sigma}\, dt \tag{35}$$

$$\text{and,} \quad \sigma^n = \sigma(t_n), \text{ (similarly for } \varepsilon \text{ and } \varepsilon_{vp}) \tag{36}$$

Since $\dot{\varepsilon}_{vp}$ is given by Equation 10, we will approximate $\Delta\varepsilon_{vp}$ by a Crank-Nicolson (12) time integration, i.e.,

$$\Delta\varepsilon_{vp} = \Delta t((1 - \theta)\dot{\varepsilon}_{vp}^n + \theta\dot{\varepsilon}_{vp}^{n+1}) \tag{37}$$

where θ = adjustable integration parameter ($0 \leq \theta \leq 1$)

If we choose $\theta = 0$, Equation 37 is equivalent to a simple forward difference scheme (Euler Method). This is also called an explicit method because we estimate $\Delta\varepsilon_{vp}$ based only on information ($\dot{\varepsilon}^n_{vp}$) at the start of the time step. As a consequence, Δt is restricted in size to avoid numerical instability (13). Alternatively, if we choose $\theta > 0$, the method is called implicit since $\Delta\varepsilon_{vp}$ depends on information at the beginning and end of the time step, generally requiring an iterative solution procedure within the time step. For $\theta \geq 1/2$, the implicit methods are unconditionally stable (14) so that the choice of Δt is governed by desired accuracy, not stability.

Returning to Equation 34, with $\Delta\varepsilon_{vp}$ replaced by Equation 37 and performing the E^{-1} operation, we have a numerical version of the viscoplastic constitutive relation which becomes exact as $\Delta t \to 0$,

$$E^{-1}(\Delta\sigma) = \Delta\varepsilon - \Delta t((1-\theta)\dot{\varepsilon}^n_{vp} + \theta\dot{\varepsilon}^{n+1}_{vp}) \tag{38}$$

Also we have the side relations valid at all time;

$$\dot{\varepsilon}_{vp} = \gamma\phi(f)\,\mathrm{sgn}(\sigma) \tag{39}$$

$$f = \sigma - k(\varepsilon_{vp}) \tag{40}$$

$$\varepsilon_{vp} = \varepsilon - E^{-1}(\sigma) \tag{41}$$

We now consider an iterative solution procedure for Equation 38 when strain loading is specified, i.e. $\Delta\varepsilon$ is known at each step. At time t_n the quantities σ^n, $\dot{\varepsilon}^n_{vp}$, and ε^n_{vp} are known, and the objective is to determine these quantities at time t_{n+1}. For brevity, we assume the elastic modulus is constant at least within the time step so that $E^{-1}(\Delta\sigma) = E^{-1}\sigma^{n+1} - E^{-1}\sigma^n$. Thus, regrouping Equation 38 with unknowns on the left we have the form:

$$P(\sigma^{n+1}) = q^n \tag{42}$$

where

$$P(\sigma^{n+1}) = E^{-1}\sigma^{n+1} + \Delta t\theta\,\dot{\varepsilon}^{n+1}_{vp} \tag{43}$$

$$q^n = \Delta\varepsilon - \Delta t(1-\theta)\dot{\varepsilon}^n_{vp} + E^{-1}\sigma^n \tag{44}$$

When $\theta > 0$, Equation 42 is a nonlinear algebraic equation in σ^{n+1} because in general $\dot{\varepsilon}_{vp}^{n+1}$ is nonlinearly related to σ^{n+1}. However, choosing $\theta = 0$ (explicit method) results in a linear equation (but at the expense of accuracy and stability concerns).

Using a Newton-Raphson procedure to solve Equation 42 (which will converge on the first iteration if $\theta = 0$), we let:

$$\sigma^{n+1} = \sigma^{i} + \delta\sigma^{i} \tag{45}$$

where σ^{i} = some estimate of σ^{n+1} at iteration i (first estimate is $\sigma^{i=1} = \sigma^{n}$).

$\delta\sigma^{i}$ = correction to estimate σ^{i}

Thus we have $P(\sigma^{i} + \delta\sigma^{i}) = q^{n}$ which when expanded in a first order Taylor series gives an estimate of the correction $\delta\sigma^{i}$:

$$P'(\sigma^{i})\delta\sigma^{i} = q^{n} - P(\sigma^{i}) \tag{46}$$

where $$P(\sigma^{i}) = E^{-1}\sigma^{i} + \Delta t\theta\dot{\varepsilon}_{vp}^{i} \tag{47}$$

and, $$P'(\sigma^{i}) = \frac{\partial P(\sigma^{i})}{\partial\sigma} = E^{-1} + \Delta t\theta\gamma \frac{\partial\dot{\varepsilon}_{vp}}{\partial\sigma} \tag{48}$$

The process is repeated with $\sigma^{i+1} = \sigma^{i} + \delta\sigma^{i}$ to get $\delta\sigma^{i+1}$, and so on until $\delta\sigma^{i+1} \to 0$.

Table 1 summarizes the above numerical solution algorithm for strain loading. A stress loading algorithm is easily established in a similar manner.

Table 1. Solution algorithm for one-dimensional viscoplasticity with strain loading.

1. Given: ε^n, σ^n, ε_{vp}^n, $\dot{\varepsilon}_{vp}^n$, P^n, P'^n (at time t_n) and ε^{n+1}

2. Time loop: $n \rightarrow n+1$ up to nmax

   (set) $q = \varepsilon^{n+1} - \varepsilon^n - \Delta t(1-\theta)\dot{\varepsilon}_{vp}^n + E^{-1}\sigma^n$

3. Iteration loop: $i = 1,2, \ldots$ imax

   (solve) $\delta\sigma^i = (P'^i)^{-1}(q - P^i)$

   (update) $\sigma^{i+1} = \sigma^i + \delta\sigma^i$

   $\varepsilon_{vp}^{i+1} = \varepsilon^{n+1} - E^{-1}\sigma^{i+1}$

   $f^{i+1} = f(\sigma^{i+1}, \varepsilon_{vp}^{i+1})$

   $\dot{\varepsilon}_{vp}^{i+1} = \gamma\phi(f^{i+1})\ \mathrm{sgn}(\sigma^{i+1})$

   $P^{i+1} = E^{-1}\sigma^{i+1} + \Delta t\theta\dot{\varepsilon}_{vp}^{i+1}$

   $P'^{i+1} = E^{-1} + \Delta t\theta \frac{\partial}{\partial\sigma}(\dot{\varepsilon}_{vp}^{i+1})$ *

4. Repeat iteration (step 3) unless one of the following conditions are satisfied:

   (a) $\vartheta = 0$ (explicit solution)

   (b) f^n and $f^{i+1} < 0$ (elastic space)

   (c) $|\delta\sigma_i| <$ tolerance (converged solution)

   (d) $i >$ imax (maximum iteration limit)

5. Print results, return to step 2 if $n <$ nmax

6. End.

* $\frac{\partial}{\partial\sigma}(\dot{\varepsilon}_{vp}^{i+1}) = \gamma\phi'(f^{i+1})\ (1 - E^{-1}\ k'(\varepsilon_{vp}^{i+1})\ \mathrm{sgn}(\sigma^{i+1}))$

MULTI-DIMENSIONAL VISCOPLASTICITY

We now consider a general viscoplastic constitutive model for continuum bodies with six-dimensional stress and strain vectors ordered as:

$$\underset{\sim}{\sigma} = \langle \sigma_{11}, \sigma_{22}, \sigma_{33}, \sigma_{12}, \sigma_{13}, \sigma_{23} \rangle^T \tag{49}$$

$$\underset{\sim}{\varepsilon} = \langle \varepsilon_{11}, \varepsilon_{22}, \varepsilon_{33}, \gamma_{12}, \gamma_{13}, \gamma_{23} \rangle^T \tag{50}$$

In point of fact, the general viscoplastic formulation is only a small extention of the one-dimensional formulation, so that the following development is presented with minimal additional discussion.

Constitutive Development. Two fundamental assumptions are as follows:

$$\underset{\sim}{\sigma} = \underline{\underline{D}}(\underset{\sim}{\varepsilon}_e) \tag{51}$$

$$\underset{\sim}{\varepsilon} = \underset{\sim}{\varepsilon}_e + \underset{\sim}{\varepsilon}_{vp} \tag{52}$$

where $\underset{\sim}{\varepsilon}_e$ = elastic strain vector

$\underset{\sim}{\varepsilon}_{vp}$ = viscoplastic strain vector

$\underline{\underline{D}}$ = elastic constitutive matrix (operator)
(and $\underline{\underline{D}}^{-1}$ is assumed to exist)

The viscoplastic strain rate is assumed to be of the Perzyna type (7) defined by:

$$\dot{\underset{\sim}{\varepsilon}}_{vp} = \gamma \phi(f) \underset{\sim}{m} \tag{53}$$

where, $$\phi(f) = \begin{cases} \phi(f), & f > 0 \\ 0, & f \leq 0 \end{cases} = \text{viscous flow function} \tag{54}$$

$$f = f(\underset{\sim}{\sigma}, \underset{\sim}{\varepsilon}_{vp}) = \text{yield function} \tag{55}$$

$$\underset{\sim}{m} = \left.\frac{\partial f}{\partial \underset{\sim}{\sigma}}\right|_{(\varepsilon_{vp} \text{ held constant})} = \text{vector gradient of f w.r.t. } \underset{\sim}{\sigma} \qquad (56)$$

and, γ = fluidity parameter (57)

Note the above relationships are identical in form to the one-dimensional relationships wherein $\underset{\sim}{m}$ replaces sgn(σ), defining the vector direction of $\dot{\underset{\sim}{\varepsilon}}_{vp}$.

The yield function f may be taken as any valid plasticity yield function with the following understanding. In six dimensional stress space all states of $\underset{\sim}{\sigma}$ giving $f(\underset{\sim}{\sigma}, \underset{\sim}{\varepsilon}_{vp}) = 0$ forms a "static yield surface" (e.g. a classical plasticity yield surface), all states of $\underset{\sim}{\sigma}$ giving $f(\underset{\sim}{\sigma}, \underset{\sim}{\varepsilon}_{vp}) = \beta > 0$ forms a "dynamic yield surface", and all states $\underset{\sim}{\sigma}$ such that $f(\underset{\sim}{\sigma}, \underset{\sim}{\varepsilon}_{vp}) < 0$ implies $\underset{\sim}{\sigma}$ is in the elastic domain, i.e., $\phi(f) = 0$ so that $\dot{\underset{\sim}{\varepsilon}}_{vp} = \underset{\sim}{0}$.

Two typical forms of the viscoplastic flow function, ϕ, given by Perzyna are:

$$\phi(f) = \left(\frac{f}{f_0}\right)^N \qquad (58)$$

$$\phi(f) = \exp\left(\frac{f}{f_0}\right)^N - 1 \qquad (59)$$

where N = exponent (material parameter)

f_0 = some normalizing parameter so that ϕ is dimensionless (material parameter)

Equation 58 is directly analogous to the form adopted in the one-dimensional development and is apparently the most popular form for soils. The second form (Equation 59) is sometimes used for metals. A series generalization of these two forms may be written as:

$$\phi(f) = \sum_{j=1}^{N} A_j \left(\frac{f}{f_0}\right)^j \qquad (60)$$

$$\phi(f) = \sum_{j=1}^{N} B_j \left(\exp\left(\frac{f}{f_0}\right)^j - 1\right) \qquad (61)$$

where A_j, B_j are additional material constants.

Having established the fundamental assumptions, the viscoplastic constitutive relationship (i.e. a set of differential equations in time relating $\underset{\sim}{\sigma}$ and $\underset{\sim}{\varepsilon}$) can be readily derived by first combining Equations 51 and 52 in rate form to get:

$$\dot{\underset{\sim}{\sigma}} = \underline{\underline{D}}(\dot{\underset{\sim}{\varepsilon}} - \dot{\underset{\sim}{\varepsilon}}_{vp}) \tag{62}$$

Upon replacing $\dot{\underset{\sim}{\varepsilon}}_{vp}$ with Equation 53, the final constitutive form is:

$$\dot{\underset{\sim}{\sigma}} = \underline{\underline{D}}(\dot{\underset{\sim}{\varepsilon}} - \gamma\phi(f)\underset{\sim}{m}) \tag{63}$$

Here it is understood that if f is a hardening yield function, then $\underset{\sim}{\varepsilon}_{vp}$ is an argument (i.e. $f = f(\underset{\sim}{\sigma}, \underset{\sim}{\varepsilon}_{vp})$). But, since $\underset{\sim}{\varepsilon}_{vp} = \underset{\sim}{\varepsilon} - \underline{\underline{D}}^{-1}(\underset{\sim}{\sigma})$, Equation 63 implicitly infers the desired $(\underset{\sim}{\sigma},\underset{\sim}{\varepsilon})$ relationship.

A numerical solution strategy, paralleling the one-dimensional procedure, is given next.

Numerical Algorithm. As in the one-dimensional case, we seek a solution $\underset{\sim}{\sigma}(t)$ when $\underset{\sim}{\varepsilon}(t)$ is specified, or vice versa. In either case, we integrate Equation 62 over one time step t_n to t_{n+1} and denote the result by:

$$\Delta\underset{\sim}{\sigma} = \underline{\underline{D}}(\Delta\underset{\sim}{\varepsilon} - \Delta\underset{\sim}{\varepsilon}_{vp}) \tag{64}$$

where
$$\Delta\underset{\sim}{\alpha} = \underset{\sim}{\alpha}^{n+1} - \underset{\sim}{\alpha}^{n} = \int_{t_n}^{t_n + \Delta t} \dot{\underset{\sim}{\alpha}}\, dt \tag{65}$$

$$\underset{\sim}{\alpha}^{n} = \underset{\sim}{\sigma}(t_n),\ \underset{\sim}{\varepsilon}(t_n),\ \text{or}\ \underset{\sim}{\varepsilon}_{vp}(t_n) \tag{66}$$

Quantities $\underset{\sim}{\alpha}^{n}$ are presumed to be known at the start of each step.

Using the previously described Crank-Nicolson time integration scheme for approximating $\Delta\underset{\sim}{\varepsilon}_{vp}$, we have $(0 \leq \theta \leq 1)$:

$$\Delta\underset{\sim}{\varepsilon}_{vp} = \Delta t((1 - \theta)\, \dot{\underset{\sim}{\varepsilon}}^{n}_{vp} + \theta\dot{\underset{\sim}{\varepsilon}}^{n+1}_{vp}) \tag{67}$$

Inserting the above into Equation 64 (after performing the $\underline{\underline{D}}^{-1}$ operation) an incremental approximation for the viscoplastic constitutive relationship is obtained (becoming exact as $\Delta t \to 0$);

$$\underline{\underline{D}}^{-1}(\Delta\underline{\sigma}) = \Delta\underline{\varepsilon} - \Delta t((1-\theta)\dot{\underline{\varepsilon}}_{vp}^{n} + \theta\dot{\underline{\varepsilon}}_{vp}^{n+1}) \tag{68}$$

Implied in the above are the viscoplastic model assumptions valid for all time:

$$\dot{\underline{\varepsilon}}_{vp} = \gamma\phi(f)\underline{m} \tag{69}$$

$$\underline{\varepsilon}_{vp} = \underline{\varepsilon} - \underline{\underline{D}}^{-1}(\underline{\sigma}) \tag{70}$$

For the case when strain loading is specified, Equation 68 is regrouped with unknowns at time t_{n+1} on left;

$$\underline{P}(\underline{\sigma}^{n+1}) = \underline{q}^{n} \tag{71}$$

where

$$\underline{P}(\underline{\sigma}^{n+1}) = \underline{\underline{D}}^{-1}\underline{\sigma}^{n+1} + \Delta t\theta\,\dot{\underline{\varepsilon}}_{vp}^{n+1} \tag{72}$$

$$\underline{q}^{n} = \Delta\underline{\varepsilon} - \Delta t(1-\theta)\dot{\underline{\varepsilon}}_{vp}^{n} + \underline{\underline{D}}^{-1}\underline{\sigma}^{n} \tag{73}$$

Here it is assumed the elastic matrix is constant (at least within the time step).

If implicit integration is employed ($\theta > 0$), Equation 71 represents a set of nonlinear algebraic equations for $\underline{\sigma}^{n+1}$. Using a Newton-Raphson procedure we let $\underline{\sigma}^{n+1} = \underline{\sigma}^{i} + \delta\underline{\sigma}^{i}$ where $\underline{\sigma}^{i}$ is some estimate of $\underline{\sigma}^{n+1}$ and $\delta\underline{\sigma}^{i}$ is a correction. An approximation for $\delta\underline{\sigma}^{i}$ is achieved by expanding $\underline{P}(\underline{\sigma}^{i} + \delta\underline{\sigma}^{i})$ in a first order Taylor Series, and solving:

$$\underline{\underline{P}}'(\underline{\sigma}^{i})\delta\underline{\sigma}^{i} = \underline{q}^{n} - \underline{P}(\underline{\sigma}^{i}) \tag{74}$$

where the Jacobian matrix $\underline{\underline{P}}'$ is:

$$\underline{\underline{P}}'(\underline{\sigma}^{i}) = \frac{\partial\underline{P}(\underline{\sigma}^{i})}{\partial\underline{\sigma}} \tag{75}$$

and

$$\underline{P}(\underline{\sigma}^{i}) = \underline{\underline{D}}^{-1}\underline{\sigma}^{i} + \Delta t\theta\dot{\underline{\varepsilon}}_{vp}^{i} \tag{76}$$

The process is repeated with $\underset{\sim}{\sigma}^{i+1} = \underset{\sim}{\sigma}^{i} + \delta\underset{\sim}{\sigma}^{i}$ to get $\delta\underset{\sim}{\sigma}^{i+1}$ and so on, until $|\delta\underset{\sim}{\sigma}| \simeq 0$. Table 2 summarizes the algorithm for strain loading.

For the case of stress loading, a similar solution procedure is readily derived to iteratively determine $\underset{\sim}{\varepsilon}^{n+1} = \underset{\sim}{\varepsilon}^{i} + \delta\underset{\sim}{\varepsilon}^{i}$, i.e.;

$$\hat{\underline{\underline{P}}}'(\underset{\sim}{\varepsilon}^{i})\delta\underset{\sim}{\varepsilon}^{i} = \hat{\underset{\sim}{q}}^{n} - \hat{\underset{\sim}{P}}(\underset{\sim}{\varepsilon}_{i}) \tag{77}$$

where
$$\hat{\underset{\sim}{q}}^{n} = \underline{\underline{D}}^{-1}\Delta\underset{\sim}{\sigma} + \Delta t(1-\theta)\dot{\underset{\sim}{\varepsilon}}^{n}_{vp} \tag{78}$$

$$\hat{\underset{\sim}{P}}(\underset{\sim}{\varepsilon}^{i}) = \underset{\sim}{\varepsilon}^{i} - \theta\Delta t\dot{\underset{\sim}{\varepsilon}}^{i}_{vp} \tag{79}$$

$$\hat{\underline{\underline{P}}}'(\underset{\sim}{\varepsilon}^{i}) = \frac{\partial\hat{\underset{\sim}{P}}(\underset{\sim}{\varepsilon}^{i})}{\partial\underset{\sim}{\varepsilon}} \tag{80}$$

The solution procedure for stress loading is summarized in Table 3. Note the solution procedure for stress loading is very similar to the strain loading procedure wherein $\underset{\sim}{q}$, $\underset{\sim}{P}$, and $\underline{\underline{P}}'$ are replaced by $\hat{\underset{\sim}{q}}$, $\hat{\underset{\sim}{P}}$, and $\hat{\underline{\underline{P}}}'$.

The complete Jacobian matrix $\underline{\underline{P}}'$ (or $\hat{\underline{\underline{P}}}'$ for stress loading) is generally nonsymmetric when hardening is included in the yield function. This may be avoided by not including contributions to the Jacobian matrix arising from partial derivatives of $f(\underset{\sim}{\sigma}, \underset{\sim}{\varepsilon}_{vp})$ w.r.t. $\underset{\sim}{\varepsilon}_{vp}$ as illustrated below.

Equation 75 defines the complete Jacobian $\underline{\underline{P}}'$ with the understanding that the hardening argument in $f(\underset{\sim}{\sigma}, \underset{\sim}{\varepsilon}_{vp})$ is to be replaced by $\underset{\sim}{\varepsilon}_{vp} = \underset{\sim}{\varepsilon} - \underline{\underline{D}}^{-1}\underset{\sim}{\sigma}$, so that the complete Jacobian matrix is:

$$\underline{\underline{P}}' = \underline{\underline{D}}^{-1} + \gamma\theta\Delta t[\phi'\underset{\sim}{m}(\underset{\sim}{m} + \underset{\sim}{h})^{T} + \phi\ (\underline{\underline{m}}' + \underline{\underline{h}}')^{T}] \tag{81}$$

where
$$\phi' = [\frac{\partial\phi}{\partial f}] \tag{82}$$

$$\underset{\sim}{m} = \{\frac{\partial f}{\partial\underset{\sim}{\sigma}}\} \tag{83}$$

$$\underline{\underline{m}}' = [\frac{\partial\underset{\sim}{m}}{\partial\underset{\sim}{\sigma}}] \quad \text{(symmetric)} \tag{84}$$

$$\underset{\sim}{h} = \underline{\underline{D}}^{-1}\{\frac{\partial f}{\partial\underset{\sim}{\varepsilon}_{vp}}\} \tag{85}$$

Table 2. Solution algorithm for general viscoplastic model with strain loading.

1. Given: $\underset{\sim}{\varepsilon}^n, \underset{\sim}{\sigma}^n, \underset{\sim}{\varepsilon}_{vp}^n, \dot{\underset{\sim}{\varepsilon}}_{vp}^n, \underset{\sim}{P}^n, \underset{\sim}{P}'^n$ (at time t_n), and $\underset{\sim}{\varepsilon}^{n+1}$.

2. Time loop: $n \rightarrow n+1$, up to nmax

   (set) $\underset{\sim}{q}^n = (\underset{\sim}{\varepsilon}^{n+1} - \underset{\sim}{\varepsilon}^n) - \Delta t(1-\theta)\dot{\underset{\sim}{\varepsilon}}_{vp}^n + \underline{\underline{D}}^{-1}\underset{\sim}{\sigma}^n$

3. Iteration loop: $i = 1,2, \ldots$ imax

   (solve): $\underline{\underline{P}}'^i \, \delta\underset{\sim}{\sigma}^i = \underset{\sim}{q}^n - \underset{\sim}{P}^i$

   (update): $\underset{\sim}{\sigma}^{i+1} = \underset{\sim}{\sigma}^i + \delta\underset{\sim}{\sigma}^i$

   $$\underset{\sim}{\varepsilon}_{vp}^{i+1} = \underset{\sim}{\varepsilon}^{n+1} - \underline{\underline{D}}^{-1}\underset{\sim}{\sigma}^{i+1}$$

   $$f^{i+1} = f(\underset{\sim}{\sigma}^{i+1}, \underset{\sim}{\varepsilon}_{vp}^{i+1})$$

   $$\underset{\sim}{m}^{i+1} = \left[\frac{\partial f^{i+1}}{\partial \underset{\sim}{\sigma}}\right]$$

   $$\dot{\underset{\sim}{\varepsilon}}_{vp}^{i+1} = \gamma\phi(f^{i+1})\,\underset{\sim}{m}^{i+1}$$

   $$\underset{\sim}{P}^{i+1} = \underline{\underline{D}}^{-1}\underset{\sim}{\sigma}^{i+1} + \Delta t\theta\dot{\underset{\sim}{\varepsilon}}_{vp}^{i+1}$$

   $$\underline{\underline{P}}'^{i+1} = \left[\frac{\partial \underset{\sim}{P}^{i+1}}{\partial \underset{\sim}{\sigma}}\right] \quad *$$

4. Repeat iteration (step 3) unless one of the following is satisfied

   (a) $\theta = 0$, (explicit integration)

   (b) f^n and $f^{i+1} < 0$, (elastic space)

   (c) $\delta\underset{\sim}{\sigma}^i$ < tolerance, (converged solution)

   (d) $i >$ imax , (iteration limit)

5. Print results, return to step 2 if $n <$ nmax

6. End

*Symmetric form of Jacobian matrix is (see Equation 87):

$$\underline{\underline{P}}' = \underline{\underline{D}}^{-1} + \gamma\theta\Delta t[\phi' \, \underset{\sim}{m} \, \underset{\sim}{m}^T + \phi \, \underline{\underline{m}}']$$

Table 3. Solution algorithm for general viscoplastic model with stress loading.

1. Given: $\underset{\sim}{\varepsilon}^n$, $\underset{\sim}{\sigma}^n$, $\dot{\underset{\sim}{\varepsilon}}^n_{vp}$, $\underset{\sim}{\varepsilon}^n_{vp}$, $\hat{\underset{\sim}{P}}^n$, $\hat{\underline{\underline{P}}}'^n$ (at time t_n), and $\underset{\sim}{\sigma}^{n+1}$

2. Time loop: n → n+1, up to nmax

   (set) $\hat{\underset{\sim}{q}}^n = \underline{\underline{D}}^{-1}(\underset{\sim}{\sigma}^{n+1} - \underset{\sim}{\sigma}^n) + \Delta t(1-\theta)\dot{\underset{\sim}{\varepsilon}}^n_{vp} + \underset{\sim}{\varepsilon}^n$

3. Iteration loop: i = 1,2 ... imax

   (solve): $\hat{\underline{\underline{P}}}'^i \, \delta\underset{\sim}{\varepsilon}^i = \hat{\underset{\sim}{q}}^n - \hat{\underset{\sim}{P}}^i$

   (update): $\underset{\sim}{\varepsilon}^{i+1} = \underset{\sim}{\varepsilon}^i + \delta\underset{\sim}{\varepsilon}^i$

   $\underset{\sim}{\varepsilon}^{i+1}_{vp} = \underset{\sim}{\varepsilon}^{i+1} - \underline{\underline{D}}^{-1}\underset{\sim}{\sigma}^{n+1}$

   $f^{i+1} = f(\underset{\sim}{\sigma}^{n+1}, \underset{\sim}{\varepsilon}^{i+1}_{vp})$

   $\underset{\sim}{m}^{i+1} = \left\{\dfrac{\partial f^{i+1}}{\partial \underset{\sim}{\sigma}}\right\}$

   $\dot{\underset{\sim}{\varepsilon}}^{i+1}_{vp} = \gamma\phi(f^{i+1})\,\underset{\sim}{m}^{i+1}$

   $\hat{\underset{\sim}{P}}^{i+1} = \underset{\sim}{\varepsilon}^{i+1} - \Delta t\theta\dot{\underset{\sim}{\varepsilon}}^{i+1}_{vp}$

   $\hat{\underline{\underline{P}}}'^{,i+1} = \left[\dfrac{\partial \hat{\underset{\sim}{P}}^{i+1}}{\partial \underset{\sim}{\varepsilon}}\right]$ *

4. Repeat iteration (step 3) unless one of the following is satisfied:
   (a) $\theta = 0$, (explicit integration)
   (b) f^n and $f^{i+1} < 0$, (elastic space)
   (c) $|\delta\underset{\sim}{\varepsilon}^{i+1}|$ < tolerance , (convergence solution)
   (d) i > imax , (iteration limit)

5. Print results, return to step 2 if n < nmax.

6. End

* Symmetric form of Jacobian is identify matrix, $\hat{\underline{\underline{P}}}' = \underline{\underline{I}}$, thus the "solve" step is trivial and $\hat{P}'$ need not be formed.

$$\underline{\underline{h}}' = \underline{\underline{D}}^{-1}\left[\frac{\partial \underline{m}}{\partial \underline{\varepsilon}_{vp}}\right] \qquad \text{(non symmetric)} \tag{86}$$

and all the above partials are taken with the other variables held constant.

If $f = f(\underline{\sigma})$, implying no hardening, then $\underline{\underline{P}}'$ becomes a symmetric matrix because $\underline{h}$ and $\underline{h}'$ are zero. Otherwise $\underline{\underline{P}}'$ has nonsymmetric contributions from the matrices $\underline{m}\ \underline{h}^T$ and $\underline{h}'^T$. By retaining only the symmetric terms to define $\underline{\underline{P}}'$ we have:

$$\underline{\underline{P}}' = \underline{\underline{D}}^{-1} + \gamma\theta\Delta t[\phi'\ \underline{m}\ \underline{m}^T + \phi\ \underline{\underline{m}}'] \tag{87}$$

In a similar development for stress loading, we find $\hat{\underline{\underline{P}}}'$ is composed of the identity matrix plus nonsymmetric matrices related to hardening. Retaining only the symmetric identity matrix we have:

$$\hat{\underline{\underline{P}}}' = \underline{\underline{I}} \tag{88}$$

In closing this section it is emphasized that the symmetric forms of the Jacobian matrices (Equations 87 and 88) are complete and correct for non hardening yield functions. For the more general case of hardening, the symmetric forms may be used with the consequence that the Newton-Raphson rate of convergence and the domain of convergence (i.e. step size) may be reduced. Of course once a converged solution is obtained, it is correct.

As illustrated in the last section of this report, the inverse of the Jacobian matrix becomes the "constitutive matrix" in forming finite element stiffness matrices. Thus the motivation for retaining the symmetric form is apparent with regard to equation solving.

SPECIALIZATION OF VISCOPLASTIC MODEL TO CAP75

Functional Forms. The foregoing viscoplastic algorithm presented in Table 2 (or Table 3 for stress loading) is specialized by identifying the functional forms for elastic, viscous, and plastic components, i.e. $\underline{D}$, $\phi(f)$, and $f(\underset{\sim}{\sigma}, \underset{\sim}{\varepsilon}_{vp})$ along with the hardening function associated with f.

In program VPDRVR (Appendix) the following forms are included:

(1) An isotropic elastic matrix is formulated with a bulk and shear modulus (K and G) whose values may change between load steps but are assumed constant within the load step, i.e.;

$$\underline{D} = \underline{D}(K,G)^n \tag{89}$$

(2) Two options for $\phi(f)$ are (see Equations 58, 59):

$$\phi(f) = \begin{cases} (f/f_0)^N \\ \text{(or)} \\ \exp\,(f/f_0)^N - 1 \end{cases} \tag{90}$$

therefore,

$$\phi'(f) = \begin{cases} N\phi(f)/f_0 \\ \text{(or)} \\ N(\phi(f) + 1)\, f^{N-1}/f_0{}^N \end{cases} \tag{91}$$

(3) A somewhat general form for $f(\underset{\sim}{\sigma}, \underset{\sim}{\varepsilon}_{vp})$ applicable to CAP75 as well as most other plasticity models is:

$$f(\underset{\sim}{\sigma}, \underset{\sim}{\varepsilon}_{vp}) = g_1(J_1, \underset{\sim}{\varepsilon}_{vp}) + g_2(J_2) \tag{92}$$

where g_1 = specified function of J_1 and $\underset{\sim}{\varepsilon}_{vp}$ where $\underset{\sim}{\varepsilon}_{vp}$ implies hardening.

g_2 = specified function of J_2.

J_1 = first invariant of stress.

J_2 = second invariant of deviator stress.

In a later section specific forms for g_1 and g_2 are given for the CAP75 plasticity model where we allow g_1 and g_2 to be specified differently in different regions of J_1, J_2 space (e.g. failure surface and cap).

The advantage of the above form for f is that the gradient vector $\underline{m}$ and the Jacobian matrix $\underline{P}'$ (symmetric form) can be established once and for all in terms of g_1 and g_2 and their derivatives as shown below.

Beginning with the stress invariant definitions:

$$J_1 = \sigma_{11} + \sigma_{22} + \sigma_{33} \tag{93}$$

$$J_2 = \frac{1}{2}(S_{11}^2 + S_{22}^2 + S_{33}^2 + 2\sigma_{12}^2 + 2\sigma_{13}^2 + 2\sigma_{23}^2) \tag{94}$$

$$\text{where} \quad S_{ii} = \sigma_{ii} - J_1/3, \quad i = 1,2,3 \quad \text{(no sum)} \tag{95}$$

we have for $\underline{m} = \partial f/\partial \underline{\sigma}$:

$$\underline{m} = g_1' \underline{b} + g_2' \underline{a} \tag{96}$$

$$\text{where} \quad g_1' = \frac{\partial g_1}{\partial J_1} \tag{97}$$

$$g_2' = \frac{\partial g_2}{\partial J_2} \tag{98}$$

$$\underline{b} = \partial J_1/\partial \underline{\sigma} = \langle 1\ 1\ 1\ 0\ 0\ 0 \rangle^T \tag{99}$$

$$\underline{a} = \partial J_2/\partial \underline{\sigma} = \langle S_{11}\ S_{22}\ S_{33}\ 2\sigma_{12}\ 2\sigma_{13}\ 2\sigma_{23} \rangle^T \tag{100}$$

And after some manipulation, $\underline{P}'$ (Equation 87) may be written as:

$$\underline{P}' = \underline{D}^{-1} + \gamma\Delta t(X_1[\underline{a}\,\underline{a}^T] + X_2[\underline{b}\,\underline{a}^T + \underline{a}\,\underline{b}^T] + X_3[\underline{b}\,\underline{b}^T] + X_4[\frac{\partial \underline{a}}{\partial \underline{\sigma}}]) \tag{101}$$

$$\text{where} \quad X_1 = b'(g_2')^2 + bg_2'' \tag{102}$$

$$X_2 = b'g_1'g_2' \tag{103}$$

$$X_3 = \varphi' (g_1')^2 + \phi g_1'' \tag{104}$$

$$X_4 = \phi g_2' \tag{105}$$

with,
$$g_1'' = \frac{\partial g_1'}{\partial J_1} \tag{106}$$

$$g_2'' = \frac{\partial g_2'}{\partial J_2} \tag{107}$$

and,
$$\left[\frac{\partial \underset{\sim}{a}}{\partial \underset{\sim}{\sigma}}\right] = \frac{1}{3}\begin{bmatrix} 2 & -1 & -1 & 0 & 0 & 0 \\ & 2 & -1 & 0 & 0 & 0 \\ & & 2 & 0 & 0 & 0 \\ \text{sym.} & & & 6 & 0 & 0 \\ & & & & 6 & 0 \\ & & & & & 6 \end{bmatrix} \tag{108}$$

Thus to change yield functions, we merely specify new functions for g_1 and g_2 with g_1', g_1'', g_2', and g_2''. Of course, hardening parameters must be maintained separately in updating the g_1 function.

CAP75 Yield Function. We now specialize Equation 92 for a particular version of the CAP75 plasticity soil model (1). Figure 2 shows the CAP75 yield function which is composed of a nonhardening "failure surface" f_F and a hardening "Cap surface" f_C. The failure surface is defined as:

$$f_F = g_{F_1}(J_1) + g_{F_2}(J_2) \tag{109}$$

where
$$g_{F_1} = -A + C \exp(BJ_1) \tag{110}$$

$$g_{F_2} = (J_2)^{1/2} \tag{111}$$

A,B,C = material constants

Note the so-called "von Mises transition" is not included in this development, and the ad hoc "tension cutoff" technique (1) is not suitable in a viscoplastic context (see Summary).

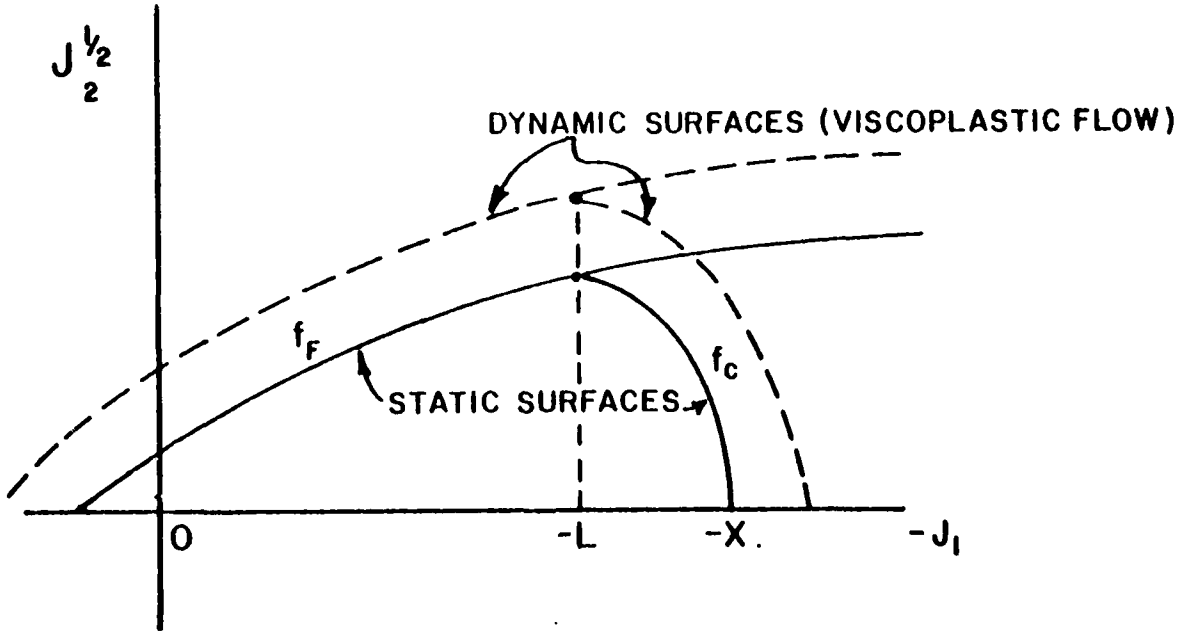

$$f_F = g_{F_1}(J_1) + g_{F_2}(J_2) = \text{FAILURE YIELD FUNCTION}$$

$$f_C = g_{C_1}(J_1, \bar{\epsilon}_{vp}) + g_{C_2}(J_2) = \text{CAP YIELD FUNCTION}$$

Figure 2. Illustration of CAP75 yield surfaces.

The cap surface, forming an ellipse quadrant, is defined as:

$$f_C = g_{C_1}(J_1, \bar{\varepsilon}) + g_{C_2}(J_2) \tag{112}$$

where,

$$g_{C_1} = (-(X - L)^2 + (J_1 - L)^2)/f_0 R^2 \tag{113}$$

$$g_{C_2} = J_2/f_0 \tag{114}$$

and,

$\bar{\varepsilon}$ = volumetric viscoplastic strain hardening function

R = ratio of principal ellipse radii

L = current location on J_1 axis of cap-failure intersection

X = current location of cap intersection on J_1 axis ($X < L$)

f_0 = normalizing constant with units of stress.

Note, f_C is a "squared" form of the cap surface presented by Sandler (1). This is necessary because during viscoplastic flow ($J_1 < X$) we must have $f_C > 0$ which is not possible with the Sandler form. Accordingly, f_0 is used to retain the units of stress for f_C.

Continuity of the hardening cap and failure surfaces (static) are maintained by the relationship;

$$X = L + R\, g_{F_1}(L) \tag{115}$$

which establishes the current ellipse quadrant of the cap surface. Typically, the ellipse ratio R is assumed constant but may be a function of L.

CAP75 Hardening Function. Hardening of the cap is given by a relationship between X and $\bar{\varepsilon}$;

$$\bar{\varepsilon} = W(e^{DX} - 1) \tag{116}$$

where W and D are positive material constants.

The strain hardening function $\bar{\varepsilon}$ is a measure of accumulated volumetric viscoplastic strain. For both rocks and soils, $\bar{\varepsilon}$ can only increase negatively

during viscoplastic loading of the cap, inferring X and L grow negatively expanding the cap during hardening. Thus the incremental update of $\bar{\varepsilon}$, when $J_1 \leq L$, is:

$$\bar{\varepsilon}^{n+1} = \bar{\varepsilon}^{n} + \min(0, \Delta\omega) \tag{117}$$

where $$\Delta\omega = \omega^{n+1} - \omega^{n} \tag{118}$$

$$\omega = \varepsilon_{vp_{11}} + \varepsilon_{vp_{22}} + \varepsilon_{vp_{33}} \tag{119}$$

For soils only, $\bar{\varepsilon}$ is allowed to be updated with positive increments of $\Delta\omega$ during viscoplastic loading of the failure surface, inferring that X and L become less negative. This retracts the cap, however the retraction is limited such that $L \leq J_1$. Sandler claims this is tantamount to kinematic hardening, not strain softening. The purpose of this procedure is to limit excessive dilatancy for soil models (i.e., subsequent compression loading will activate the cap sooner). Thus the incremental update of $\bar{\varepsilon}$ for soils, when $J_1 > L$, is:

$$\bar{\varepsilon}^{n+1} = \min\ (\bar{\varepsilon}_a, \bar{\varepsilon}_c) \tag{120}$$

where $$\bar{\varepsilon}_a = \bar{\varepsilon}^{n} + \max\ (0, \Delta\omega) \tag{121}$$

$$\bar{\varepsilon}_c = W(e^{DX_c} - 1) \tag{122}$$

$$X_c = J_1 + Rg_{F_1}(J_1) \tag{123}$$

In the above, $\bar{\varepsilon}_c$ insures that $L \leq J_1$. Also, $\bar{\varepsilon}^{n+1}$ is never allowed to become greater than its initial value.

Table 4 summarizes the implementation of the CAP75 plasticity model. The procedure in Table 4 should be viewed as a subroutine which internally maintains the hardening parameters $\bar{\varepsilon}$, X, and L. The subroutine outputs g_1, g_1', g_1'' and g_2, g_2', g_2'' which allows calculation of f, $\underline{m}$, and $\underline{P}'$ by Equations 92, 96, and 101, respectively. These, in turn provide the necessary ingredients in Table 2 (or Table 3 without $\underline{P}'$) for the general viscoplastic algorithm.

Table 4. CAP75 hardening update and g_1, g_2 computations.

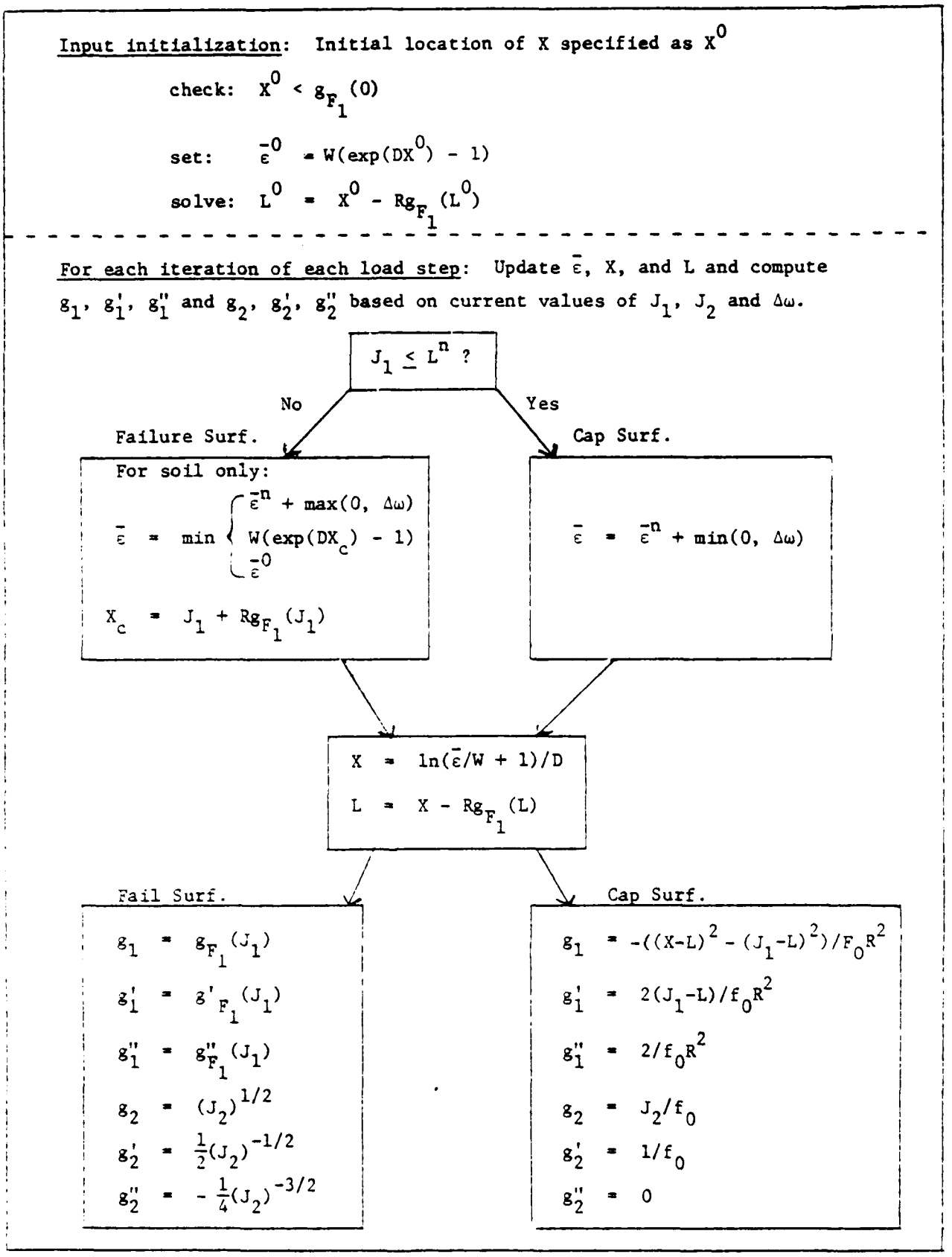

EXAMPLE RESULTS AND DISCUSSION

In this section the CAP75 viscoplastic model is studied for two loading conditions; uniaxial strain and triaxial stress. In both cases the plasticity parameters are taken from Sandler (1) representing McCormick Ranch Sand. Table 5 gives the values of the model parameters used for both loading conditions along with three values for the fluidity parameter.

The intent of these examples is to verify the viscoplastic algorithm and to illustrate the effect of the fluidity parameter, γ, on the time dependent responses. The three values of the fluidity parameter (γ = 0.001, 0.01, and 0.1) were chosen to produce responses with varying amounts of viscoplastic flow.

With regard to numerical time integration, each example problem is solved within 1% relative accuracy for five choices of the Crank-Nicolson θ parameter; θ = 0.0, 0.25, 0.50, 0.75, and 1.0. That is, for each choice of θ, the time step size, Δt, is repeatedly halved until successive solutions agree within 1%, thus providing an efficiency comparison.

Uniaxial strain. Figure 3 shows the uniaxial strain loading history for the strain component ε_{11}, all other strain components are zero. Here, ε_{11} increases in compression at a constant rate, held constant, unloaded at a constant rate, and finally held constant so that eventually stress responses would approach steady state for all γ. Note the units of time are not and need not be explicitly stated since they are the reciprocal of whatever units are assumed for γ.

Figure 4 shows the corresponding σ_{11} stress response for the three magnitudes of γ. For the relatively large magnitude, γ = 0.1, the response is nearly inviscid throughout the entire loading history. In other words, the viscous element (see Figure 1) has very little effect in retarding the plastic response so that the solution is nearly elasto-plastic. Indeed, the steady state σ_{11} values agree exactly with the inviscid CAP75 plasticity solution (17), thereby, providing a verification of the viscoplastic solution. If higher values of γ were used, the response would not change significantly, and the small peaks at time = 1.0 and 5.5 would be flattened, resulting in a perfectly inviscid solution.

Table 5. Viscoplastic model parameters

Elastic Parameters	Bulk Modulus = 66.67 ksi Shear Modulus = 40.0 ksi
CAP75 Plastic* (McCormick Ranch Sand)	Failure Surface (Equation 109): A = 0.25, B = 0.67, C = 0.18 Cap Surface (Equation 112): R = 2.5, f_o = 0.25, X^o = -0.1888 Cap Hardening (Equation 116): W = 0.066, D = 0.67
Viscous Parameters	Flow Function (Equation 90a) N = 1, f_o = 0.25 Fluidity parameter γ = 0.001, 0.01, and 0.1

*Units: A, C, f_o and X^o = ksi; B and D = ksi^{-1}, γ = $time^{-1}$;
R, W, and N are dimensionless.

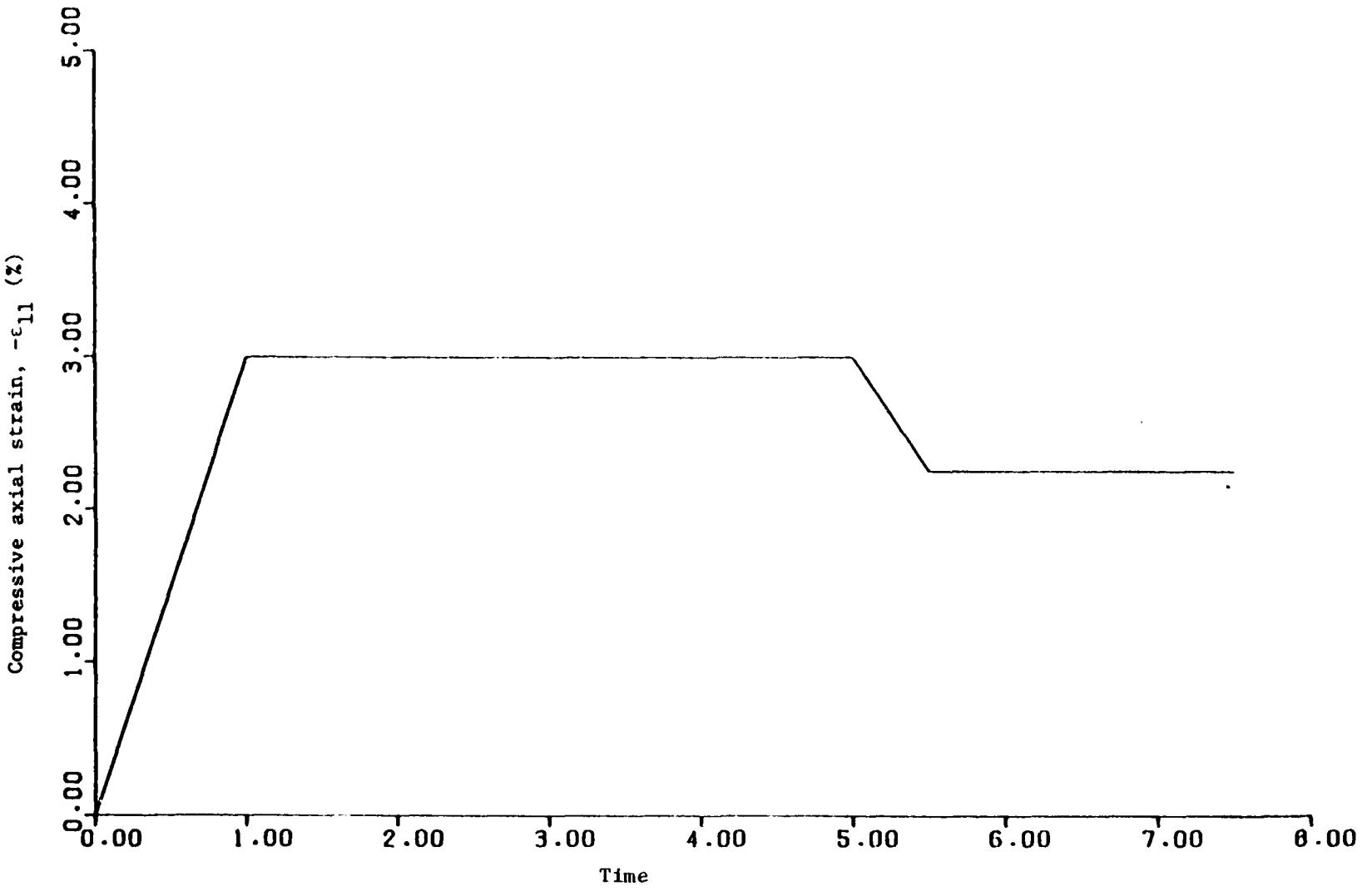

Figure 3. Uniaxial strain loading schedule.

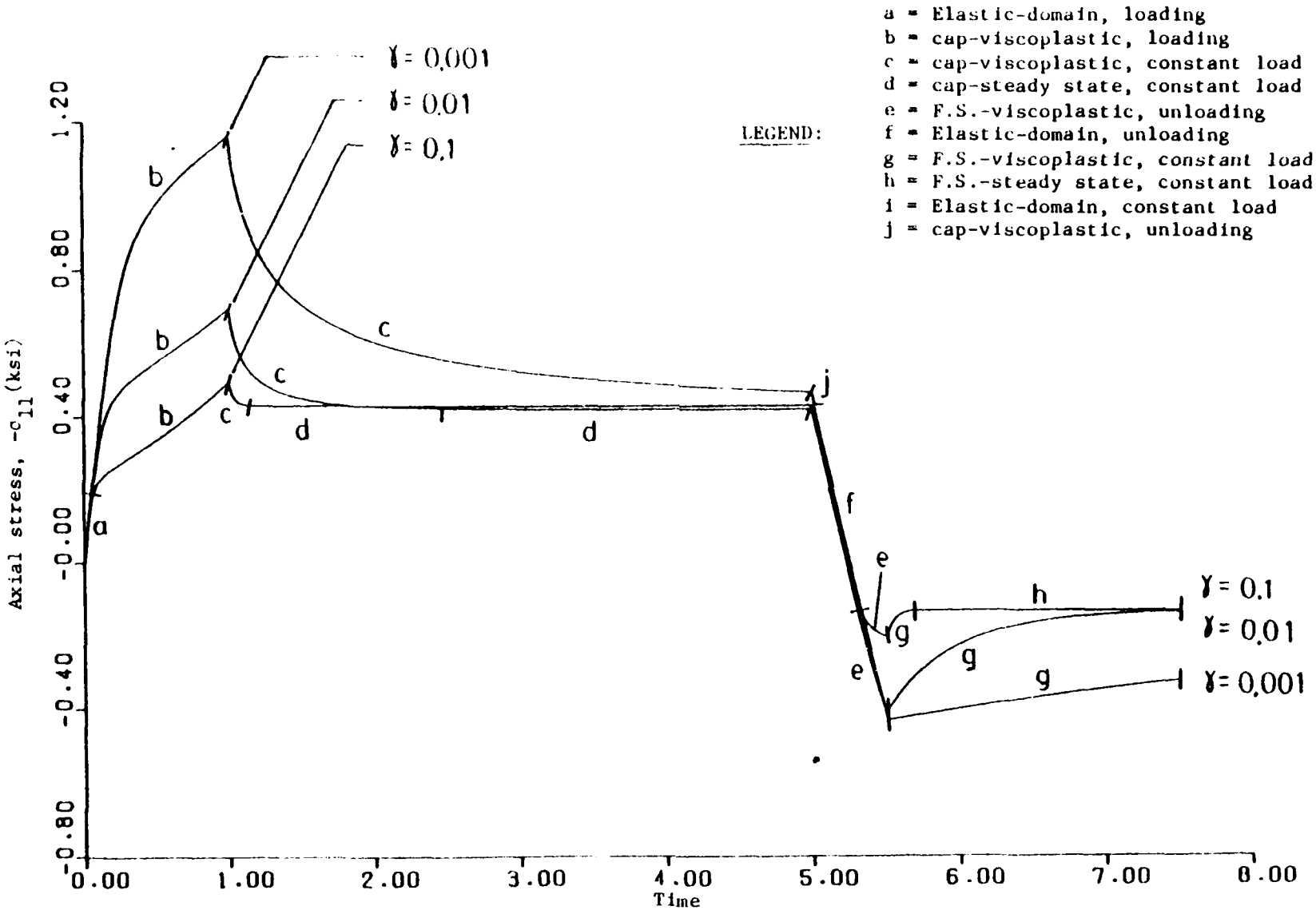

Figure 4. Axial stress response.

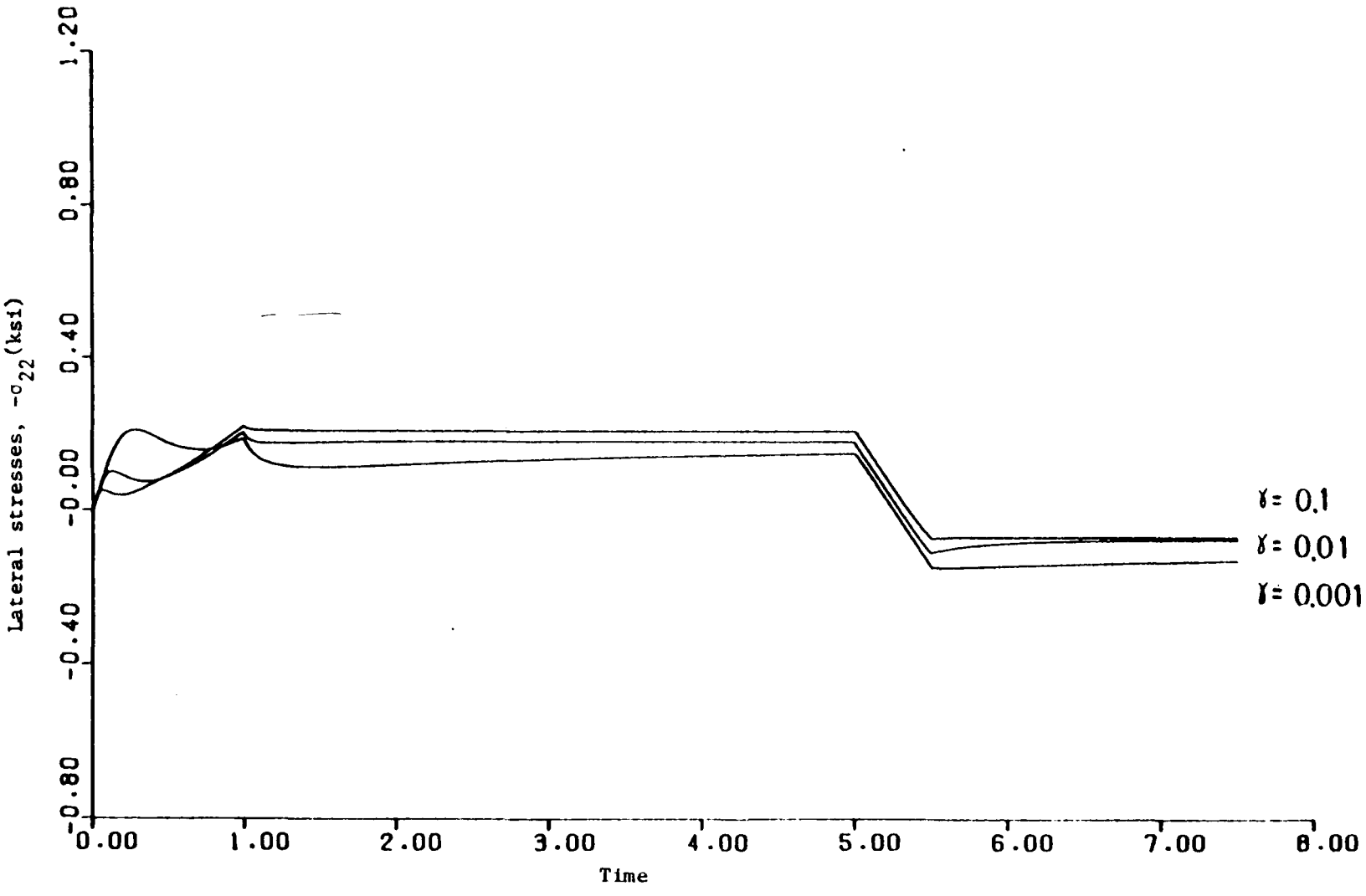

Figure 5. Lateral stress response ($\sigma_{22} = \sigma_{33}$)

For the relatively small magnitude, $\gamma = 0.001$, Figure 4 shows a pronounced viscous effect such that steady state conditions are not reached within the constant loading duration, and peak stress magnitudes far exceed the maximum stresses achievable from the inviscid plasticity solution. The rate of stress relaxation decreases with decreasing values of γ. In the limit as $\gamma \to 0$, the response becomes perfectly elastic in which case the shape of the σ_{11} response history would be similar to the ε_{11} loading history.

For reference, Figure 4 also indicates which CAP75 regions (i.e. failure surface, cap surface, or elastic domain) are being activated during the loading schedule. Lateral stress responses ($\sigma_{22} = \sigma_{33}$) are shown in Figure 5.

The foregoing solutions were independently obtained for five choices of θ, each requiring a certain minimum value of Δt to achieve relative accuracy within 1%. Table 6a shows the required values of Δt to maintain accuracy (Note, although not necessary, Δt was taken uniformly throughout the loading schedule). In general it is observed that $\theta = 0.5$ permits the largest time step, in some cases up to four times greater than $\theta = 0.0$ or $\theta = 1.0$. Surprisingly, the influence of γ on Δt is small. That is, within the range $0.001 \leq \gamma \leq 0.1$, Δt for accuracy changes at most by a factor of two. This is not in conformance with initial expectations wherein it was incorrectly anticipated that Δt for accuracy would be inversely proportional to γ. In other words, it was presumed the dimensionless product $\gamma\Delta t$ would be an accuracy measure.

It is now conjectured that the accuracy requirement for Δt is predominantly controlled by the loading schedule, i.e., Δt must be sufficiently small to adequately capture the abrupt changes in loading rates. This contention is supported by the observation that the greatest accuracy deviations throughout the loading schedule occurred at changes in loading rates, primarily at time = 1.0.

Lastly, the Δt values in Table 6a for the conditionally stable algorithms, $\theta = 0.0$ and 0.25, are controlled strictly by accuracy not stability. Unstable values of Δt were typically found to be an order of magnitude or more than the accuracy controlled values at Δt. Unstable solutions are readily distinguished by wild oscillations of the responses.

Triaxial Stress. Figure 6 shows the triaxial stress loading schedule. Initially, hydrostatic loading ($\sigma_{11} = \sigma_{22} = \sigma_{33}$) is applied at a constant rate

Table 6a. Uniaxial strain: required Δt for accuracy

Integration Parameter θ	Fluidity Parameter		
	$\gamma = 0.001$	$\gamma = 0.01$	$\gamma = 0.1$
0.00	0.00625	0.0125	0.00625
0.25	0.00625	0.025	0.0125
0.50	0.025	0.025	0.0125
0.74	0.00625	0.0125	0.0125
1.00	0.00625	0.0125	0.00625

Table 6b. Triaxial stress: required Δt for accuracy

Integration Parameter θ	Fluidity Parameter		
	$\gamma = 0.001$	$\gamma = 0.01$	$\gamma = 0.1$
0.00	0.050	0.0125	0.00625
0.25	0.10	0.025	0.0125
0.50	0.10	0.05	0.025
0.75	0.05	0.025	0.0125
1.00	0.025	0.0125	0.00625

and then held constant. Next, while holding the lateral stresses constant, the axial stress, σ_{11}, is increased at a constant rate, held constant, unloaded at a constant rate, and finally held constant at hydrostatic pressure.

The corresponding axial strain response is shown in Figure 7 for the three magnitudes of γ. As in the previous example, the relatively high magnitude, $\gamma = 0.1$, produces a nearly inviscid elasto-plastic response history. Accordingly, large amounts of plastic straining is observed. Conversely for the relatively low magnitude, $\gamma = 0.001$, rapid plastic straining is impeded resulting in smaller strain magnitudes. In the limit as $\gamma \to 0$, the strain response would be purely elastic. Figure 8 shows the corresponding response histories for the lateral strains ($\varepsilon_{22} = \varepsilon_{33}$).

Table 6b lists the minimum values of Δt to achieve accuracy within 1% for the five choices of θ. As before, $\theta = 0.5$ is the most efficient choice for maintaining accuracy with maximum Δt. Further it can be observed that the influence of γ is fairly uniform. That is, for any value of θ, Δt generally decreases by one half for each magnitude increase in γ.

Summarizing both examples, the following observations are noted:

1. For $\gamma >> 0.1$, the responses are inviscid (elasto-plastic). For $\gamma << 0.001$ the responses are elastic.
2. For all γ, $\theta = 0.5$ is most efficient with regard to maintaining accuracy with largest Δt.
3. In the range, $0.001 \leq \gamma \leq 0.1$, the fluidity parameter has less influence on the required Δt for accuracy than anticipated. Loading rates and changes in loading rates are presumed to be the major factor for the Δt accuracy requirement.
4. For $\theta < 0.5$ (conditional stability), the Δt required for accuracy is significantly less than the Δt limit for stability.

It is emphasized that the above observations pertain only to the example problems presented herein.

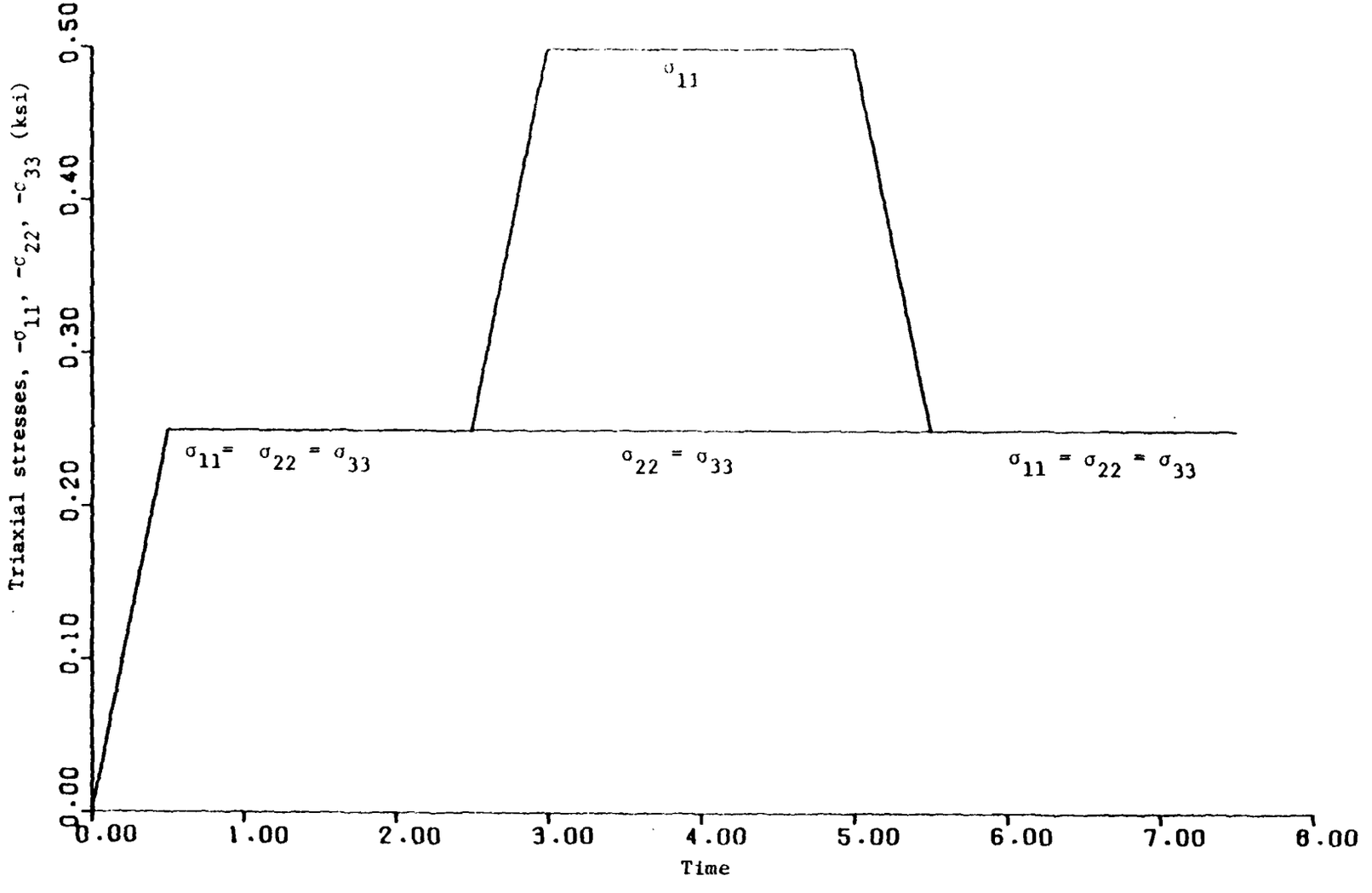

Figure 6. Triaxial stress loading schedule.

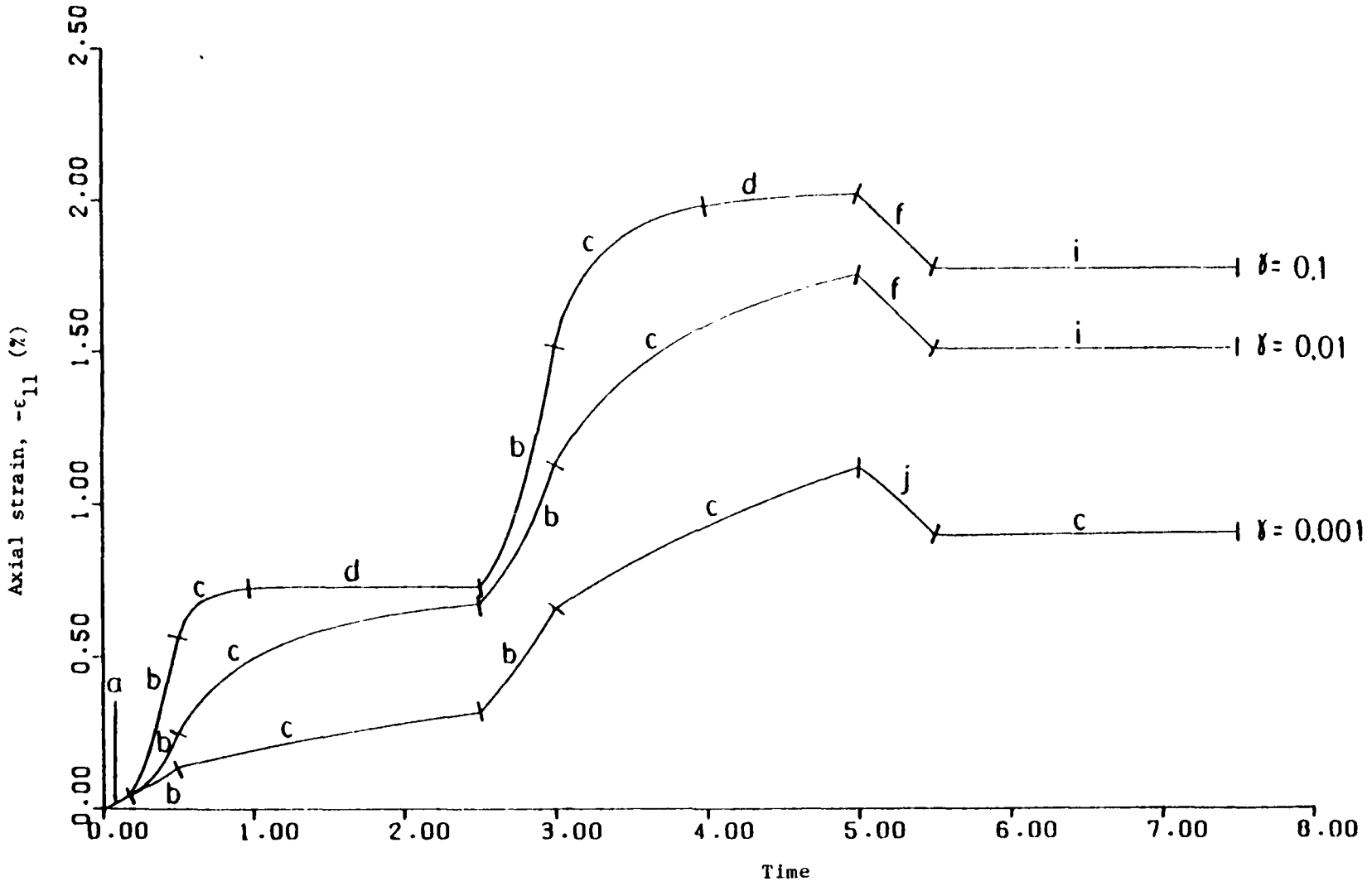

Figure 7. Axial strain response.

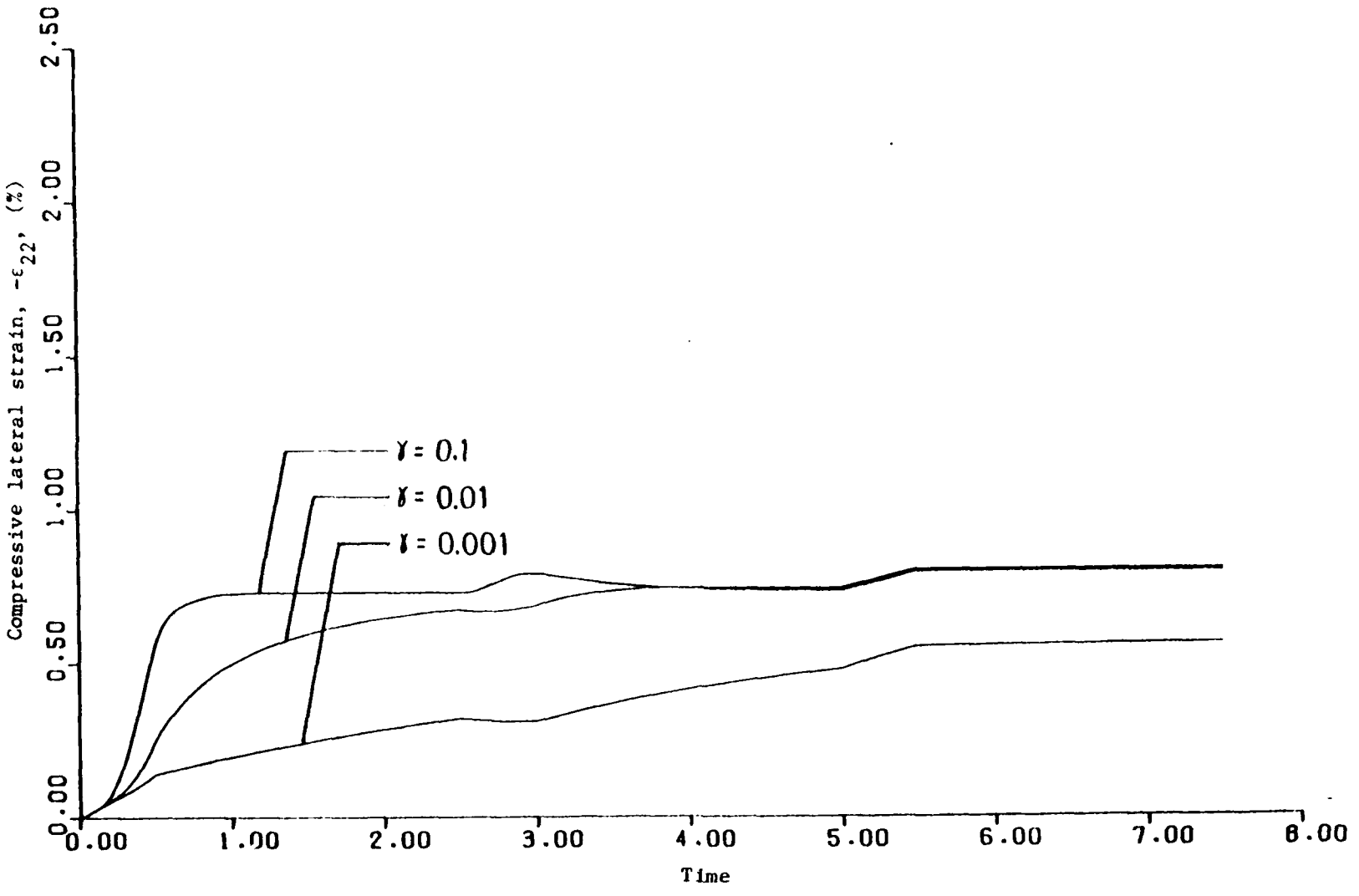

Figure 8. Lateral strain response ($\varepsilon_{22} = \varepsilon_{33}$)

EXTENSION TO FEM APPLICATIONS

For the sake of completeness, this section illustrates how to incorporate the general viscoplastic constitutive model into a quasi-static, finite element displacement formulation.

Using standard FEM notation, the global equilibrium equations to be satisfied at any time t_{n+1} are:

$$\int_V \underline{\underline{B}}^T \underset{\sim}{\sigma}^{n+1} \, dV = \underset{\sim}{F}^{n+1} \tag{124}$$

with $$\underset{\sim}{\varepsilon} = \underline{\underline{B}} \, \underset{\sim}{u} \tag{125}$$

where $\underline{\underline{B}}$ = strain-displacement matrix

$\underset{\sim}{u}$ = nodal point displacements

$\underset{\sim}{F}$ = nodal force vector (body, traction, and point loads)

V = volume of body

Since $\underset{\sim}{\sigma}^{n+1}$ is the unknown in Equation 124, we follow a procedure paralleling Table 2 for strain loading, the only difference being that strain is not a priori specified but determined iteratively via displacements. To this end we let;

$$\underset{\sim}{\sigma}^{n+1} = \underset{\sim}{\sigma}^{i} + \delta\underset{\sim}{\sigma}^{i} \tag{126}$$

$$\underset{\sim}{\varepsilon}^{n+1} = \underset{\sim}{\varepsilon}^{i} + \delta\underset{\sim}{\varepsilon}^{i} \tag{127}$$

where $\underset{\sim}{\sigma}^{i}$, $\underset{\sim}{\varepsilon}^{i}$ = estimates of $\underset{\sim}{\sigma}^{n+1}$, $\underset{\sim}{\varepsilon}^{n+1}$ at iteration i.

$\delta\underset{\sim}{\sigma}^{i}$, $\delta\underset{\sim}{\varepsilon}^{i}$ = correction to estimate $\underset{\sim}{\sigma}^{i}$, $\underset{\sim}{\varepsilon}^{i}$.

Thus, the equilibrium equation may be written as:

$$\int_V \underline{\underline{B}}^T \delta\underset{\sim}{\sigma}^{i} \, dV = \delta \, \underset{\sim}{F}^{i} \tag{128}$$

with $$\delta\underset{\sim}{F}^{i} = \underset{\sim}{F}^{n+1} - \int_V \underline{\underline{B}}^T \underset{\sim}{\sigma}^{i} \, dV \tag{129}$$

Note when $\underset{\sim}{\sigma}^{i} = \underset{\sim}{\sigma}^{n+1}$, we have $\delta\underset{\sim}{F}^{i} = \underset{\sim}{0}$.

From Equation 74 we have a relationship for $\delta\underset{\sim}{\sigma}^i$:

$$\underline{P}'\,\delta\underset{\sim}{\sigma}^i = (\delta\underset{\sim}{\varepsilon}^i + \underset{\sim}{\varepsilon}^i - \underset{\sim}{\varepsilon}^n) - \underline{D}^{-1}(\underset{\sim}{\sigma}^i - \underset{\sim}{\sigma}^n) - \Delta t((1-\theta)\dot{\underset{\sim}{\varepsilon}}^n_{vp} + \theta\dot{\underset{\sim}{\varepsilon}}^i_{vp}) \quad (130)$$

Or more simply (noting $\underset{\sim}{\varepsilon}_{vp} = \underset{\sim}{\varepsilon} - \underline{D}^{-1}\underset{\sim}{\sigma}$):

$$\delta\underset{\sim}{\sigma}^i = \underline{C}^i\,(\delta\underset{\sim}{\varepsilon}^i + \delta\underset{\sim}{q}^i) \quad (131)$$

where $$\delta\underset{\sim}{q}^i = (\underset{\sim}{\varepsilon}^i_{vp} - \underset{\sim}{\varepsilon}^n_{vp}) - \Delta t((1-\theta)\dot{\underset{\sim}{\varepsilon}}^n_{vp} + \theta\dot{\underset{\sim}{\varepsilon}}^i_{vp}) \quad (132)$$

$$\underline{C}^i = [P'(\underset{\sim}{\sigma}^i)]^{-1} \quad \text{Jacobian inverse} \quad (133)$$

In Equation 132, both groups of terms defining $\delta\underset{\sim}{q}^i$ are estimates of the increment $\Delta\underset{\sim}{\varepsilon}_{vp}$ when these estimates agree (converged solution), we have $\delta\underset{\sim}{q}^i = 0$.

Upon inserting Equation 131 into Equation 128 with $\delta\underset{\sim}{\varepsilon}^i = \underline{B}\delta\underset{\sim}{u}^i$, the iterative-global-equilibrium equation becomes:

$$\underline{K}^i\,\delta\underset{\sim}{u}^i = \delta\underset{\sim}{F}^i - \delta\underset{\sim}{Q}^i \quad (134)$$

where $$\underline{K}^i = \int_V \underline{B}^T\,\underline{C}^i\,\underline{B}\,dV \quad (135)$$

$$\delta\underset{\sim}{Q}^i = \int_V \underline{B}^T\,\underline{C}^i\,\delta\underset{\sim}{q}^i\,dV \quad (136)$$

As the number of iterations increases ($i \to \infty$), we have $\underset{\sim}{\sigma}^i = \underset{\sim}{\sigma}^{n+1}$, $\underset{\sim}{\varepsilon}^i = \underset{\sim}{\varepsilon}^{n+1}$, $\underset{\sim}{\varepsilon}^i_{vp} = \underset{\sim}{\varepsilon}^{n+1}_{vp}$, etc., as well as, $\delta\underset{\sim}{F}^i = \delta\underset{\sim}{q}^i = \delta\underset{\sim}{Q}^i = \delta\underset{\sim}{u}^i = \underset{\sim}{0}$, (i.e. a converged solution).

Table 7 summarizes the numerical FEM algorithm for a time step from time t_n to t_{n+1}. First iteration estimates ($i = 1$) are based on previously known values at time t_n so that we have $\underset{\sim}{\sigma}^1 = \underset{\sim}{\sigma}^n$, $\underset{\sim}{\varepsilon}^1 = \underset{\sim}{\varepsilon}^n$, $\underline{C}^1 = \underline{C}^n$, $\underline{K}^1 = \underline{K}^n$, etc. Accordingly from Equations 129 and 132, we have $\delta\underset{\sim}{F}^1 = \underset{\sim}{F}^{n+1} - \underset{\sim}{F}^n$, and $\delta\underset{\sim}{q}^1 = -\Delta t\dot{\underset{\sim}{\varepsilon}}^n_{vp}$.

Several variations of the solution strategy in Table 7 are easily established. First, for the explicit method ($\theta = 0$) we have $\underline{C}^i = \underline{D}$ resulting in linear equations that convergence in one iteration but at the expense of reduced Δt to control

1. Given at Gauss Points: $\underset{\sim}{\sigma}^n$, $\underset{\sim}{\varepsilon}^n$, $\dot{\underset{\sim}{\varepsilon}}_{vp}^n$, $\underset{\sim}{\varepsilon}_{vp}^n$, and $\underline{\underline{C}}^n$ (or reconstruct), along with global $\underline{\underline{K}}^n$.

2. Time loop: $n \rightarrow n+1$, up to nmax.

(set:) $\delta\underset{\sim}{F}^1 = \underset{\sim}{F}(t_{n+1}) - \underset{\sim}{F}(t_n)$

$\delta\underset{\sim}{q}^1 = -\Delta t \dot{\underset{\sim}{\varepsilon}}_{vp}^n$

$\delta\underset{\sim}{Q}^1 = \int_V \underline{\underline{B}}^T \underline{\underline{C}}^n \delta\underset{\sim}{q}^1 \, dV$

3. Iteration loop: $i = 1, 2, \ldots$ imax.

(solve): $\underline{\underline{K}}^i \delta\underset{\sim}{u}^i = \delta\underset{\sim}{F}^i - \delta\underset{\sim}{Q}^i$

$\delta\underset{\sim}{\varepsilon}^i = \underline{\underline{B}}^T \delta\underset{\sim}{u}^i$

(update): $\underset{\sim}{\varepsilon}^{i+1} = \underset{\sim}{\varepsilon}^i + \delta\underset{\sim}{\varepsilon}^i$

$\underset{\sim}{\sigma}^{i+1} = \underset{\sim}{\sigma}^i + \underline{\underline{C}}^i(\delta\underset{\sim}{\varepsilon}^i + \delta\underset{\sim}{q}^i)$

$\underset{\sim}{\varepsilon}_{vp}^{i+1} = \underset{\sim}{\varepsilon}_{vp}^{i+1} - \underline{\underline{D}}^{-1}\underset{\sim}{\sigma}^{i+1}$

$\dot{\underset{\sim}{\varepsilon}}_{vp}^{i+1} = \gamma\phi(f^{i+1})\,\underset{\sim}{m}^{i+1}$

$\underline{\underline{C}}^{i+1} = [\underline{\underline{P}}'^{i+1}]^{-1}$ *

$\delta\underset{\sim}{F}^{i+1} = \underset{\sim}{F}(t_{n+1}) - \int_V \underline{\underline{B}}^T \underline{\underline{C}}^{i+1} \underset{\sim}{\sigma}^{i+1} \, dV$

$\delta\underset{\sim}{q}^{i+1} = \underset{\sim}{\varepsilon}_{vp}^{i+1} - \underset{\sim}{\varepsilon}_{vp}^n - \Delta t((1-\theta)\dot{\underset{\sim}{\varepsilon}}_{vp}^n + \theta\dot{\underset{\sim}{\varepsilon}}_{vp}^{i+1})$

$\delta\underset{\sim}{Q}^{i+1} = \int_V \underline{\underline{B}}^T \underline{\underline{C}}^{i+1} \delta\underset{\sim}{q}^{i+1} \, dV$

$\underline{\underline{K}}^{i+1} = \int_V \underline{\underline{B}}^T \underline{\underline{C}}^{i+1} \underline{\underline{B}} \, dV$

4. Repeat iteration (step 3) until convergence (see Table 2).

5. Print results, return to (step 2) if $n <$ nmax.

6. End.

*$\underline{\underline{P}}' = \underline{\underline{D}}^{-1} + \gamma\theta\Delta t[\phi'\underset{\sim}{m}\,\underset{\sim}{m}^T + \phi\underline{\underline{m}}']$ (see Equation 87)

accuracy/stability. A second variation is with regard to modified or quasi Newton-Raphson methods (15). Here $\underline{K}^i$ is held constant (modified Newton-Raphson) or approximately updated in its triagularized form (quasi Newton-Raphson) for the purpose of reducing solution time per iteration but at the expense of slower convergence rates. Lastly, if the iteration process is terminated prior to convergence (or if the one-step explicit algorithm is used) the out-of-balance force $\delta\underset{\sim}{F}^{i+1}$ may be added to the applied force $\underset{\sim}{F}$ in the next time step as a "load correction" to reduce error accumulation.

For dynamic problems the acceleration vector can be numerically integrated by any suitable scheme (e.g. Newmark Beta-method) independently of the Crank-Nicolson scheme used for the viscoplastic constitutive model. In such cases, it may be presumed that Δt controlling accuracy would not be smaller than Δt required for same problem with inviscid plasticity (i.e. CAP75 without viscous effects). This is because the viscoplastic response at any instant is bracketed between a purely elastic response and an inviscid plastic response. Thus, it is reasonable to assume that Δt for a dynamic viscoplastic solution need not be less than Δt for a dynamic inviscid-plastic solution.

SUMMARY AND RECOMMENDATIONS

The viscoplastic formulation and numerical algorithm developed herein provides a general format for incorporating various plasticity models into a Perzyna-type viscoplastic constitutive relationship suitable for FEM applications. In particular, the CAP75 viscoplastic model illustrated in this report and contained in the program VPDRVR (Appendix) appears to have a sufficient generality to faithfully represent the time-dependent behavior of many geological materials over a wide range of loadings.

The VPDRVR program has been extensively checked and verified including cross-checks with the CAPDRVR program for steady state elasto-plastic solutions, as well as, self-checking time-dependent inverse solutions. Inverse solutions are obtained by taking the stress responses from a strain loading problem and using them for a stress loading problem whose strain response should match the original strain input (or vice versa). These severe self-checking tests demonstrated that the algorithm is accurate and working admirably. Furthermore, the architecture of the VPDRVR program permits relatively easy addition of new elastic, plastic and/or viscous functional forms.

Future research is needed to bring this work to full fruition. Two major areas are (1) experimental verification and parameter identification, and (2) numerical studies for optimizing efficiency/accuracy of the FEM algorithm.

The former area should be addressed first to establish the capabilities and limitations of the viscoplastic model. Existing experimental data for time-dependent behavior of soils and rocks (2,3,4,5) is primarily for slow rates of loading. Hence, it is strongly recommended to obtain additional experimental data for rapid loading rates. Concurrent with experimental verification, is the need for developing feasible parameter identification techniques. Lastly, with regard to time-dependent tension failure or damage, additional theoretical and experimental work is needed. A tension visco-damage model recently proposed by Whitman (18) shows some promise in this area.

REFERENCES

1. Sandler, I.S. and D. Rubin, "An Algorithm and a Modular Subroutine for the CAP Model," Int. Journal for Numerical and Analytical Methods in Geomechanics, Vol. 3, 1979, pp. 173-186.

2. Akai, K., T. Adachi and K. Nishi, "Mechanical Properties of Soft Rocks," IX Conference on Soil Mech. Found. Eng., Tokyo, Vol. 1, 1977, pp. 7-10.

3. Komamura, F., and J. Huang, "New Rheological Model for Soil Behavior," Journ. of the Geotech. Eng. Div., ASCE, Vol. 100, 1974, pp. 807-823.

4. Robertson, E.C., "Creep of Solenhofen Limestone Under Moderate Hydrostatic Pressure," Rock Deformation, Mem. Geol. Soc. Amer., Vol. 79, 1960, pp. 227-244.

5. Singh, A., and J.K. Mitchell, "General Stress-Strain-Time Functions for Soils," Soil Mech. and Found. Div., ASCE, Vol. 94, 1968, pp. 21-46.

6. Valanis, K.C., "A Theory of Viscoplasticity Without a Yield Surface," Archives of Mechanics, No. 23, 1971, pp. 517-555.

7. Perzyna, P., "Fundamental Problems in Viscoplasticity," Advances in Applied Mechanics, Vol. 9, 1966, pp. 244-368.

8. Katona, M.G., "Combo Viscoplasticity: An Introduction with Incremental Formulation," Computers and Structures, Vol. 11, No. 3, 1980, pp. 217-224.

9. Bodner, S.R., and V. Parton, "Constitutive Equations for Equations for Elastic-Viscoplastic Strain-Hardening Materials," Journal of Applied Mech., ASME, Vol. 42, 1975, pp. 385-389.

10. Phillips, A. and H.C. Wu, "A Theory of Viscoplasticity," Int. Journal of Solids and Structures, Vol. 9, 1973, pp. 15-30.

11. Ziekiewicz, O.C. and I.C. Cormeau, "Visco-plasticity, Plasticity and Creep in Elastic Solids - A Unified Numerical Approach," Int. Journal for Numer. Methods in Eng., Vol. 8, pp. 821-845.

12. Owen, D.R.J., and E. Hinton, "Finite Elements in Plasticity, Theory and Practice," Pineridge Press Limited, Swansea, U.K., 1980.

13. Cormeau, I., "Numerical Stability in Quasi-Static Elasto/Visco-Plasticity," Int. Journal for Numerical Methods in Eng.," Vol. 9, 1975, pp. 109-127.

14. Hughes, T.R., and R.L. Taylor, "Unconditionally Stable Algorithms for Quasi-Static Elasto/Viscoplastic Finite Element Analysis," Int. Journal Numerical Methods in Engineering. (to be published).

15. Dennis, J.R. and J.J. More, "Quasi-Newton Methods, Motivation and Theory," SIAM Review, Vol. 19, 1977, pp. 46-86.

16. Matthies, H., and G. Strang, "The Solution of Nonlinear Finite Element Equations," Int. Journal Numerical Methods in Engineering, Vol. 14, 1979, pp. 1613-1626.

17. Crawford, J., "CAPDRVR Computer Program for Exercising Plasticity Constitutive Models," CEL,NCBTC, Port Hueneme, CA, 1980.

18. Whitman, L., "Visco-Damage Tension Model of Rocks for Ground Shock Calculations," Weidlinger Associates, Report to Defense Nuclear Agency, DNA 5271F, 1980.

APPENDIX

PROGRAM VPDRVR: INSTRUCTIONS/DOCUMENTATION

This Appendix provides input instructions and documentation for the VPDRVR computer program (FORTRAN IV). VPDRVR exercises the CAP75 viscoplastic model developed in this report for general states of strain or stress loading schedules. The general solution strategy parallels the algorithm presented in Table 2 for strain loading or Table 3 for stress loading. The procedure for updating the cap hardening parameters follows the algorithm presented in Table 4.

Part I contains user input instructions. Part II describes program organization, subroutines, and program variables. Part III provides input/output for a simple benchmark problem.

Input data cards are grouped in the following categories:

A. (Cards 1 and 2): Heading and master control

B. (Cards 3,4, and 5): Elastic functions/parameters

C. (Cards 6,7,8, and 9): Plastic functions/parameters

D. (Card 10): Viscous functions/parameters

E. (Cards 11, 12): Loading schedules for stress or strain

Part I. USER INPUT INSTRUCTIONS

A. Problem Initiation, Heading and Master Control Cards.

Card 1. (15A4) Heading

Columns	Variable	Entry Description	Notes
01-60 (15A4)	TITLE	Descriptive problem title, (program terminates if TITLE(1) = STOP).	(1)

Card 2. (4I5, A1, 2F10.0) Master Controls

Columns	Variable	Entry Description	Notes
01-05 (I5)	LTYPE	Loading type identification: = 0, strain loading. = 1, stress loading.	(2)
06-10 (I5)	NTSEG	Number of time segments to define loading, (Default = 1, Maximum = 30).	(3)
11-15 (I5)	ITMAX	Number of Newton-Raphson iterations, (Default = 10).	(4)
16-20 (I5)	KPRINT	Output print control: = 0, standard response output. = 1, above plus iteration parameters = 2, above plus yield function values. = 3, above plus iterative correction vector $\geq$ 4, above plus Jacobian matrix.	(5)
20-21 (A1)	IPLOT	Plot control for response data written to unit 11: = Y, (YES) Data written to unit 11 = N, (NO) Not written	(6)
22-31 (F10.0)	THETA	Crank Nicolson integration parameter, θ; $0 \leq \theta \leq 1.0$.	(7)
32-41 (F10.0)	CONVRG	Convergence tolerance for Newton-Raphson iteration, (Default = 0.01, i.e. 1% relative error).	(8)

B. Elastic Function and Parameter Cards

Card 3. (2I5) Selection of Elastic Functions

Columns	Variable	Entry Description	Notes
01-05 (I5)	IFBMOD	Selection of bulk modulus function, $K(J_1)$: = 1, $K(J_1)$ = BDATA(1), (linear). = 2, $K(J_1)$ = BDATA(1)/(1-BDATA(2))* (1-BDATA(2)*EXP(BDATA(3)*J1) (Default = 1)	(9)
06-10 (I5)	IFSMOD	Selection of shear modulus function, $G(J_2)$: = 1, $G(J_2)$ = SDATA(1), (linear) = 2, $G(J_2)$ = SDATA(1)/(1-SDATA(2))* (1-SDATA(2)*EXP(-SDATA(3)*J2)). (Default = 1)	(10)

Card 4. (7F10.0) Bulk modulus parameters, BDATA.

Columns	Variable	Entry Description	Notes
01-10 (F10.0)	BDATA(1)	First bulk modulus parameter.	(11)
11-20 (F10.0)	BDATA(2)	Second bulk modulus parameter.	
21-30 (F10.0)	BDATA(3)	Third bulk modulus parameter.	

Card 5. (7F10.0) Shear modulus parameters, SDATA.

Columns	Variable	Entry Description	Notes
01-10 (F10.0)	SDATA(1)	First shear modulus parameter.	(12)
11-20 (F10.0)	SDATA(2)	Second shear modulus parameter.	
21-30 (F10.0)	SDATA(3)	Third shear modulus parameter.	

C. Plastic Function and Parameter Cards

Card 6. (4I5, G10.0) Selection of CAP75 functions

Columns	Variable	Entry Description	Notes
01-05 (I5)	IFFAIL	Selection of failure surface function: $f_F = \sqrt{J_2} + g_{F_1}(J_1)$: = 1, g_{F_1} = -FDATA(1) + FDATA(2)*J1. = 2, g_{F_1} = -FDATA(1) + FDATA(2)* EXP(FDATA(3)*J1). (Default = 1)	(13)
06-10 (I5)	IFCAPR	Selection of cap surface ellipse ratio R: = 0, No cap, just failure surface. = 1, R = CDATA(1). = 2, R = CDATA(1)/(1 + CDATA(2))* (1.0 + CDATA(2)*EXP(CDATA(3)*EL)).	(14)
11-15 (I5)	IFHARD	Control of cap hardening: = 0, No hardening, stationary cap. = 1, CAP75 hardening function is used: $\bar{\varepsilon}$ = W*(EXP(D*X) - 1). W = HDATA(1) D = HDATA(2)	(15)
16-20 (I5)	KAPTYP	Selection for soil or rock hardening laws: = 0, soil material. = 1, rock material.	(16)
21-30 (G10.0)	XINITL	Initial location of cap X on J_1 axis.	(17)

Card 7. (7F10.0) Failure Surface Parameters, FDATA.

Columns	Variable	Entry Description	Notes
01-10 (F10.0)	FDATA(1)	First failure surface parameter.	(18)
11-20 (F10.0)	FDATA(2)	Second failure surface parameter.	
21-30 (F10.0)	FDATA(3)	Third failure surface parameter.	

* Card 8. (7F10.0) Cap Surface Parameters for R, CDATA.

Columns	Variable	Entry Description	Notes
01-10 (F10.0)	CDATA(1)	First cap R parameter.	(19)
11-20 (F10.0)	CDATA(2)	Second cap R parameter.	
21-30 (F10.0)	CDATA(3)	Third cap R parameter.	

* Card 9. (7F10.0) Hardening cap parameters, HDATA.

Columns	Variable	Entry Description	Notes
01-10 (F10.0)	HDATA(1)	First hardening paramter, W.	(20)
11-20 (F10.0)	HDATA(2)	Second hardening parameter, D.	

---

*Skip Cards 8 and 9 if IFCAPR = 0.

D. Viscous Function and Parameter Card

Card 10. (I5, 3F10.0) Selection of viscous function/parameters

Columns	Variable	Entry Description	Notes
01-05 (I5)	IFVISC	Selection of viscous function ϕ: = 1, ϕ = (f/ANORM)**EXPN. = 2, ϕ = EXP((f/ANORM)**EXPN) - 1. (Default = 1)	(21)
06-15 (F10.0)	EXPN	Exponent in ϕ function, (Default = 1.0).	(22)
16-25 (F10.0)	GAMMA	Fluidity parameter, γ.	(23)
26-35 (F10.0)	ANORM	Normalizing constant in ϕ function, (Default = max(FDATA(1), 0.01)	(24)

E. Input Loading Schedule and Time Steps.

Repeat card set 11 and 12 NTSEG times; NS = 1, NTSEG

Card 11 (F10.0, 2I5) Time segment, number of stops, print control.

Columns	Variable	Entry Description	Notes
01-10 (F10.0)	TS(NS)	Time at end of segment NS.	(25)
11-15 (I5)	NUMDT(NS)	Number of times steps within time segment NS. (Default = 10)	(26)
16-20 (I5)	IPRNT(NS)	Print interval for standard output: = 1, every time step prints output. = n, every nth step prints. (Default = 1)	(27)

Card 12 (6F10.0) Stress or strain load vector at time TS(NS).

Columns	Variable	Entry Description	Notes
01-10 (F10.0)	PLOAD(1,NS)	σ_{11} (or ε_{11}) at TS(NS).	(28)
11-20 (F10.0)	PLOAD(2,NS)	σ_{22} (or ε_{22}) at TS(NS).	
21-30 (F10.0)	PLOAD(3,NS)	σ_{33} (or ε_{33}) at TS(NS).	
31-40 (F10.0)	PLOAD(4,NS)	σ_{12} (or ε_{12}) at TS(NS).	
41-50 (F10.0)	PLOAD(5,NS)	σ_{13} (or ε_{13}) at TS(NS).	
51-60 (F10.0)	PLOAD(6,NS)	σ_{23} (or ε_{23}) at TS(NS).	

END OF INPUT FOR ONE PROBLEM

Commentary Notes with Input Instructions:

1. Problems may be run back-to-back. Terminate the last problem by writing STOP in columns 1 to 4.

2. Strain loading implies the six components of strain will be specified individually during the loading schedule. Similarly, stress loading implies the six components of stress will be individually specified.

3. For either stress or strain loading, NTSEG is the desired number of time segments to define the loading histories in a piecewise linear fashion.

4. Generally 10 iterations is more than sufficient to achieve convergence. If convergence is not achieved, it is a strong indication that the time step is too large. Note that convergence of the Newton-Raphson procedure does not guarantee accuracy. Accuracy can only be assured by repeatable solutions with smaller time steps.

5. Standard output includes stress or strain responses, cap location, number iterations to converge, stress invariants, and type of response. For KPRINT > 0, additional information is given primarily for debugging purposes.

6. Standard response data is written to unit 11 for subsequent plotting on a CALCOMP plotter. Subroutine GRAPH is used for plotting and maybe removed or replaced if desired.

7. For THETA = 0.0, the solution algorithm is explicit resulting in linear equations (i.e. no Newton-Raphson iteration). For THETA > 0, the algorithm is implicit and generally more accurate for a given time size, but requires Newton-Raphson iteration. For THETA $\geq$ 0.5, the algorithm is unconditionally stable.

8. The convergence tolerance, CONVRG, is tested against the ratio formed by the norm of the correction vector for stress (or strain) divided by the norm of the stress (or strain) vector. Norms are Euclidean.

9. The nonlinear bulk modulus function given by IFBMOD = 2 is taken from CAPDRIVER (Reference 17). It is a function of J_1 (first stress invariant) and is treated the same for loading or unloading. Additional functions may be added to program in FUNCTION DI(I,J).

10. The nonlinear shear modulus function given by IFSMOD = 2 is a function of J_2, second deviator stress invariant (see Note 9).

11. For future program expansion, BDATA is dimensioned to 7 to allow incorporation of higher order nonlinear functions.

12. SDATA is dimensioned to 7 (see above).

13. For IFFAIL = 1, the failure surface is standard Drucker-Prager (or Von Mices if FDATA(2) = 0.0). For IFFAIL = 2, the failure surface is the exponential form suggested by Sandler for CAP75. Additional functional forms may be added to the program in FUNCTION FG1.

14. By setting IFCAPR = 0, the plasticity model is governed by only the failure surface. For IFCAPR = 1 or 2 the cap surface is included with R given by the corresponding functional form. Additional functional forms for R may be added to program in FUNCTION FRCAP. (Note for IFCAPR = 2, R = R(EL) where EL is "L" of cap).

15. If desired, a nonhardening cap surface may be used by setting IFHARD = 0. Otherwise the CAP75 hardening function is employed. New hardening functions can be employed by modifying SUBROUTINE CAP75.

16. See Table 4 for the special hardening rules for soils (KAPTYP = 0).

17. The initial location of X defines the starting position of the cap surface. The program checks that XINITL is not greater than FCUT, i.e. the intersection of the failure surface with J1 axis. If it is, XINITL is automatically reset slightly less than FCUT. Note, the so-called Von Mises Transition employed by Sandler is not included in this development. Thus, if it is desired to obtain steady-state viscoplastic solutions to exactly match CAP75 plasticity solutions, XINITL should be chosen so that the initial L location is not greater than zero.

18. The "standard Sandler" CAP75 failure surface is the form given by IFFAIL = 2. In which case FDATA(1) = A, FDATA(2) = C, and FDATA(3) = B.

19. The "standard Sandler" CAP75 cap surface parameter is the form given by IFCAPR = 1, i.e., CDATA(1) = R.

20. If IFHARD = 0, HDATA(1) and HDATA(2) are read but not used. If IFCAPR = 0, cards 8 and 9 are not read. HDATA as well as FDATA and CDATA are dimensioned to 7 for future program expansion.

21. For geological materials IFVISC = 1 is generally the most popular form for the viscous function. Additional functional forms such as Equations 60 and 61 may be added to the program in SUBROUTINE PHIF.

22. EXPN need not be a whole number, but must be greater than zero.

23. GAMMA has units of inverse time, the units (e.g. seconds, hours, years) correspond to the loading time units TS in Card 11.

24. Generally the default value of ANORM is appropriate providing FDATA(1) $\neq$ 0.0. ANORM should not be viewed as an independent material parameter since it is always associated with GAMMA in the quotient GAMMA/ANORM**EXPN.

25. Up to 30 time segments may be used to define a piecewise continuous collection of straight lines to define loading. For the first time segment, the program automatically assumes initial time is zero, i.e. TS(0) = 0.0. Thus, TS(1) is the time at the end of first segment, TS(2) is the time at the end of the second segment, etc. Successive values of TS(NS) must be greater than the previous value.

26. Any number of time steps may be assigned to each time segment. Accuracy/ stability is controlled by the time step size so that it is good practice to repeat solutions by doubling the value of NUMDT(NS). Although the time step size may be specified differently in each time segment, it is good practice not to make changes in Δt between segments by a factor of more than 2.

27. The printout interval may be specified differently for each time segment.

28. Loading values at the end of each time segment are specified individually for each vector component of strain if LTYPE = 0, or each vector component of stress if LTYPE = 1. For the first time segment the initial loading and responses are automatically assumed zero i.e., $\sigma(0) = \varepsilon(0) = 0$. Standard continuum mechanics sign convenctions are observed for all input and output. For example, if a uniaxial stress loading cycle is desired in which σ_{11} is compressed at a constant rate to a stress value -10.0, held constant, then reverse loaded at a constant rate to a tensile stress value of +1.0, and again held constant; we infer NTSEG = 4, and σ_{11} is described by:

```
PLOAD(1,1) = -10.0
PLOAD(1,2) = -10.0
PLOAD(1,3) = +1.0
PLOAD(1,4) = +1.0
```

and all other stress components (PLOAD) are zero.

PART II. VPDRVR Documentation

Table A1 describes subroutines and functions employed in VPDRVR along with associated calls. Table A2 illustrates the program flow path.

Listed below are all COMMON statements with a description of their variables:

1. COMMON/MASTER/

THETA = θ, Crank-Nicolson integration parameter
CONVRG = convergence tolerance ratio
DT = Δt, current time step size
LTYPE = loading type; strain = 0, stress = 1.
NTSEG = number of time segments
KPRINT = print control parameter
ITMAX = maximum number of Newton-Raphson iterations

2. COMMON/ELAST/

BDATA(7) = bulk modulus coefficients
SDATA(7) = shear modulus coefficients
IFBMOD = functional form of bulk modulus
IFSMOD = functional form of shear modulus

3. COMMON/PLAST/

X = cap surface location X
EL = cap surface location L
VH = $\bar{\varepsilon}$, viscoplastic volumetric strain hardening
VHMAX = $\bar{\varepsilon}_{max}$, maximum value of $\bar{\varepsilon}$
FDATA(7) = CAP75 failure surface constants
CDATA(7) = CAP75 cap surface constants
HDATA(7) = CAP75 cap hardening constants
IFFAIL = functional form of failure surface
IFCAPR = functional form of cap surface
IFHARD = functional form of cap hardening
KAPTYP = indicator for rock or soil hardening law; soil = 0, rock = 1

4. COMMON/VISCO/

EXPN = N, exponent in ϕ function
GAMMA = γ, fluidity parameter
ANORM = f_0, normalizing constant in ϕ function
IFVISC = functional form of ϕ function

5. COMMON/RESULT/

EPS(6) = $\underline{\varepsilon}$, strain vector
SIG(6) = $\underline{\sigma}$, stress vector
EVP(6) = $\underline{\varepsilon}_{vp}$, viscoplastic strain vector

EVPDOT(6) = $\dot{\underset{\sim}{\varepsilon}}_{vp}$, viscoplastic strain rate vector

SJ1 = J_1, first stress invariant

SJ2 = J_2, second deviator stress variant

ITER = iteration number

6. COMMON/LOADNG

TS(30) = time at end of time segment
PLOAD(30) = loading at end of time segment
IPRINT(30) = print interval in time segment
NUMDT(30) = number of time steps in time segment

7. COMMON/UTLTY/

P(6) = $\underset{\sim}{P}$ or $\hat{\underset{\sim}{P}}$ in Equation 72 or 79
PP(6,6) = $\underset{\sim}{P}'$, Jacobian matrix (Equation 101)
RHS(6) = q or $\hat{q}$ in Equation 73 or 78
DELCOR(6) = $\delta\underset{\sim}{\sigma}$ or $\delta\underset{\sim}{\varepsilon}$, correction vector for Newton-Raphson
DPLOAD(6) = $\Delta\underset{\sim}{\sigma}$ or $\Delta\underset{\sim}{\varepsilon}$, load increment
DEVPKK = $\Delta\omega$, increment of volumetric viscoplastic strain

8. COMMON/YIELDF/

G1 = g_1, value of plastic surface function g_1

G1P = g_1', first derivative of g_1 w.r.t. J_1

G1PP = g_1'', second derivative of g_1 w.r.t. J_1

G2 = g_2, value of plastic surface function g_2

G2P = g_2', first derivative of g_2 w.r.t. J_2

G2PP = g_2'', second derivative of g_2 w.r.t. J_2

9. COMMON/VFLOWF/

F = f_F or f_C, yield function value

PHI = ϕ, viscous function value

PHIP = ϕ', derivative of ϕ w.r.t. f

PHIPRE = ϕ^n, value of ϕ at end of previous time step

VHPRE = $\bar{\varepsilon}^n$, value of $\bar{\varepsilon}$ at end of previous time step

ISURF = indicator for governing surface: failure surface = 0, cap = 1

Table A1. Subroutines and Functions

Name	Purpose	Called by	Calls to
VPDRVR	Main program: Executive duties for controlling input calls, initialization, time step sequencing, and output.		NPUT4M LOADS GETSIG GETEPS GRAPH
NPUT4M	Reads in functional forms and parameters for elastic, plastic, and viscous components of viscoplastic model.	VPDRVR	FG1 FRCAP
LOADS	Reads in loading schedule, time step, and print controls.	VPDRVR	-
GETSIG	Determines stresses for strain loading by Newton-Raphson iteration and updates responses.	VPDRVR	SOLVER VPLAST DI
GETEPS	Determines strains for stress loading by Newton-Raphson iteration and updates responses.	VPDRVR	VPLAST DI
VPLAST	Computes stress invariants, yield function value, viscoplastic strain rate, and forms Jacobian for GETSIG.	GETSIG GETEPS	CAP75 PHIF
CAP75	Computes yield functions g_1 and g_2 and their derivatives for CAP75 plasticity and updates hardening parameters.	VPLAST	FG1 FRCAP
PHIF	Computes viscous flow function ϕ and its derivative ϕ'.	VPLAST	—
SOLVER	Gauss elimination equation solver	GETSIG	—
GRAPH	Calcomp plotting subroutine	VPDRVR	—
*DI(I,J)	Determines components of D^{-1} elastic matrix	GETSIG GETEPS	—
*FG1(SJ1,M)	Computes g_1, g_1' and g_1'' as a function first stress invariant.	NPUT4M CAP75	— —
*FRCAP(EL)	Computes cap parameter R as a function of cap location	CAP75 NPUT4M	—

*FUNCTION SUBPROGRAMS

Table A2. VPDRVR Program Flow

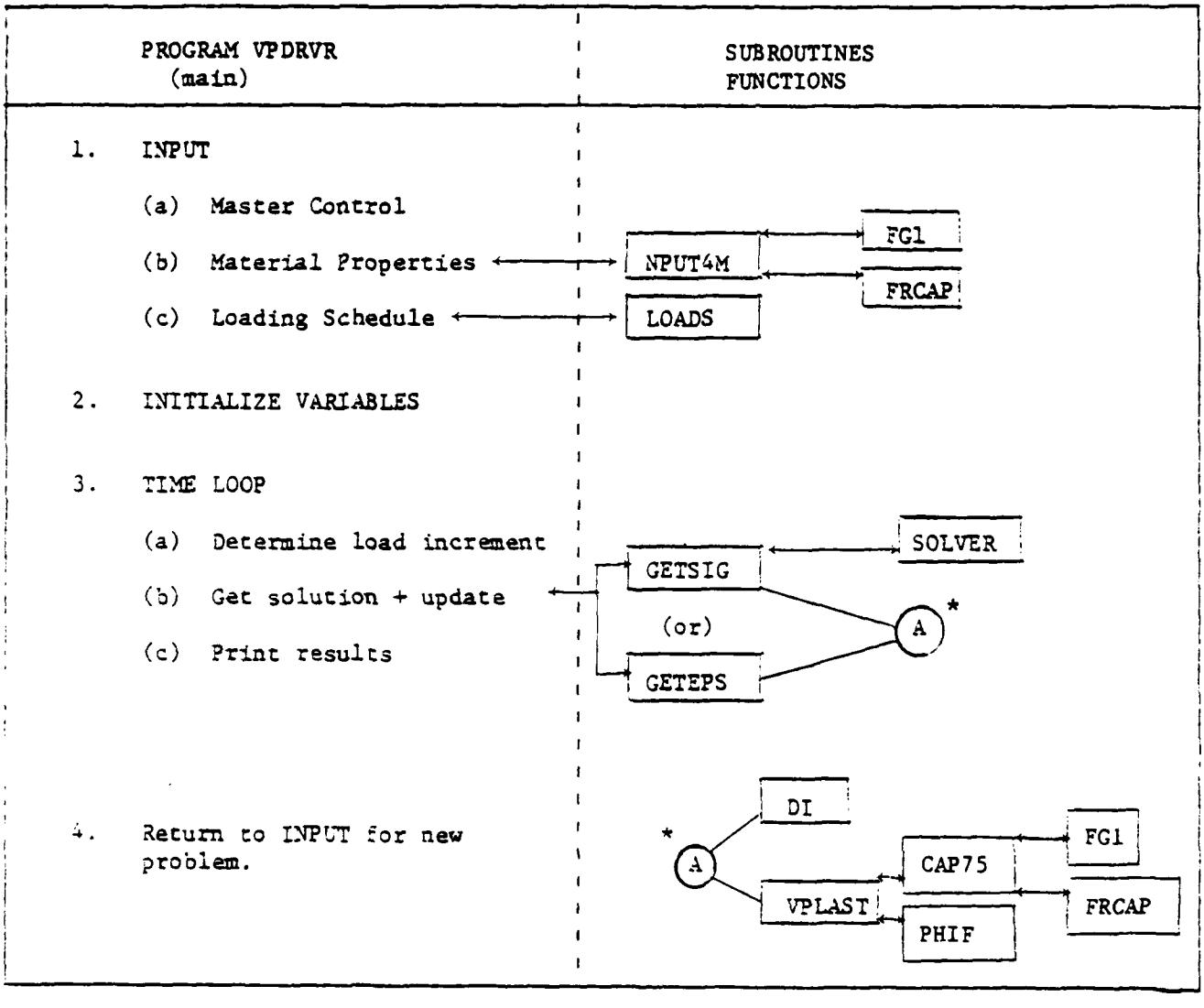

PART III Example input/output

The uniaxial strain problem presented in the main body of this report is used here as a benchmark example for the VPDRVR program. On the following page is listed the formatted input (card images) corresponding to the input instructions in Part I of this appendix. Subsequent pages show the output from the VPDRVR program including a restatement of the input with default values, as well as, response data. For brevity, the printout of response data is limited for each of the four time segments to include only the time segment midpoint and end values. All data is adequately labeled and should cause no confusion except, perhaps, for the nomenclature associated with the response "STATE". Here the following meanings are implied:

CAP-VP = viscoplastic flow above cap surface
CAP-SS = steady state response on (or near) cap surface
FSURF-VP = viscoplastic flow above failure surface
FSURF-SS = steady state response on (or near) failure surface
ELASTIC = stress state is in elastic domain

Input to VPDRVR, Uniaxial Strain, $\gamma = 0.01$.

```
00010 SAMPLE OUTPUT OF VPDRVR - UNIAXIAL STRAIN LOAD
00020      0     4           ON    .75
00030      1     1
00040 66.67
00050 40.0
00060      2     1     1     0     -.1888
00070 0.25         0.18         0.67
00080 2.5
00090 0.066        0.67
00100      1              0.01
00110 1.             80    40
00120 -0.03
00130 5.            320   160
00140 -0.03
00150 5.5            40    20
00160 -0.0225
00170 7.5           160    80
00180 -0.0225
00190 STOP
```

Output from VPDRVR (5 pages)

```
**********************************************************************
**                                                                  **
**                  REVISED CAP DRIVER, VISCOPLASTIC                **
**                                                                  **
**              * * UNIVERSITY OF NOTRE DAME, JUNE 1981 * *         **
**                                                                  **
**********************************************************************

    PROBLEM NUMBER 1
    SAMPLE OUTPUT OF VPDRVR - UNIAXIAL STRAIN LOAD


-PROBLEM CONTROL VARIABLES-

STRAIN(0) OR STRESS(1) LOAD INPUT.....  0
NUMBER OF TIME SEGMENTS DEFINING LOAD..  4
N-R ITERATION LIMIT..................... 10
PRINT CONTROL VARIABLE.................  0
PLOT CONTROL...........................  N
THETA, FOR CRANK-NICOLSON INTEGRATION..  0.7500E+00
CONVERGANCE TOLERANCE RATIO............  0.1000E-01
```

VISCOPLASTIC MATERIAL DEFINITIONS

-ELASTIC FUNCTION FORMS-

BULK MODULUS FUNCTION..... 1

SHEAR MODULUS FUNCTION..... 1

-PLASTIC FUNCTION FORMS-

FUNCTION FOR FAILURE SURFACE..... 2

FUNCTION FOR CAP SURFACE..... 1

FUNCTION FOR CAP HARDENING..... 1

CAP TYPE(SOIL(0) OR ROCK(1))..... 0

-VISCOPLASTIC FUNCTION FORM AND PARAMETERS-

FUNCTION FOR FLOW RULE..... 1

EXPONENT FOR FLOW RULE..... 0.1000E+01

FLUIDITY PARAMETER..... 0.1000E-01

NORMALIZING CONSTANT..... 0.2500E+00

-ELASTIC-PLASTIC PARAMETERS-

CONSTANT	BULK-MOD	SHEAR-MOD	FAIL-SURF	CAP-SURF	CAP HARDG
C1	0.6667E+07	0.4000E+07	0.2500E+00	0.2500E+01	0.6600E-01
C2	0.0	0.0	0.1800E+00	0.0	0.6700E+00
C3	0.0	0.0	0.6700E+00	0.0	0.0
C4	0.0	0.0	0.0	0.0	0.0
C5	0.0	0.0	0.0	0.0	0.0
C6	0.0	0.0	0.0	0.0	0.0
C7	0.0	0.0	0.0	0.0	0.0

-INITIAL CAP PARAMETERS-

INITIAL LOCATION OF CAP X..... -0.1888E+00

INITIAL LOCATION OF CAP L..... -0.1061E-01

INITIAL VOLUMETRIC HARDENING STRAIN.... -0.7842E-01

FCUT, WHERE FAILURE SURFACE IS ZERO.... 0.4901E+00

LOAD TIME HISTORY

-STRAIN VECTOR LOADING VALUES AT END OF EACH TIME SEGMENT-

SEGMENT	TSTART	TEND	STEPS	PRINT	SXX	SYY	SZZ	SXY	SXZ	SYZ
1	0.0	1.00	80	40	-0.10000E-01	0.0	0.0	0.0	0.0	0.0
2	1.00	5.00	320	160	-0.30000E-01	0.0	0.0	0.0	0.0	0.0
3	5.00	5.50	40	20	-0.22500E-01	0.0	0.0	0.0	0.0	0.0
4	5.50	7.50	160	80	-0.22500E-01	0.0	0.0	0.0	0.0	0.0

STRESS/STRAIN OUTPUT

OUTPUT HAS FORMAT:

STATE (STATE)	TIME (TIME)	ITER (ITER)	STRESS SIG(1) SIG(2) " SIG(6)	STRAIN EPS(1) EPS(2) " EPS(6)	VP-STRAIN EVP(1) EVP(2) " EVP(6)	VP-RATE EVPDOT(1) EVPDOT(2) " EVPDOT(6)	SJ1 (SJ1)	SJ2 (SJ2)	PHI (PHI)	CAP EL (EL)

RESPONSE NUMBER- 40 TIME SEGMENT- 1 TIME INCREMENT- 40 GAMMA*DT= 0.1250E-03 DT= 0.1250E-01

STATE	TIME	ITER	STRESS	STRAIN	VP-STRAIN	VP-RATE	SJ1	SJ2	PHI	CAP EL
CAP - VP	0.500	1	-0.5492E+00	-0.1530E-01	-0.9938E-02	-0.2758E-01	-0.7211E+00	0.7153E-01	0.1517E+01	-0.2658E+00
			-0.8597E-01	0.0	-0.7283E-03	0.5287E-03				
			-0.8597E-01	0.0	-0.7283E-03	0.5287E-03				
			0.0	0.0	0.0	0.0				
			0.0	0.0	0.0	0.0				
			0.0	0.0	0.0	0.0				

RESPONSE NUMBER- 80 TIME SEGMENT- 1 TIME INCREMENT- 80 GAMMA*DT= 0.1250E-03 DT= 0.1250E-01

STATE	TIME	ITER	STRESS	STRAIN	VP-STRAIN	VP-RATE	SJ1	SJ2	PHI	CAP EL
CAP - VP	1.000	1	-0.6945E+00	-0.3000E-01	-0.2407E-01	-0.2754E-01	-0.1100E+01	0.8057E-01	0.1477E+01	-0.6677E+00
			-0.2029E+00	0.0	-0.2143E-03	0.1504E-02				
			-0.2029E+00	0.0	-0.2143E-03	0.1504E-02				
			0.0	0.0	0.0	0.0				
			0.0	0.0	0.0	0.0				
			0.0	0.0	0.0	0.0				

RESPONSE NUMBER- 240 TIME SEGMENT- 2 TIME INCREMENT-160 GAMMA*DT= 0.1250E-03 DT= 0.1250E-01

STATE	TIME	ITER	STRESS	STRAIN	VP-STRAIN	VP-RATE	SJ1	SJ2	PHI	CAP EL
CAP - SS	3.000	1	-0.4213E+00	-0.3000E-01	-0.2669E-01	-0.2459E-04	-0.7842E+00	0.1917E-01	0.3457E-02	-0.7281E+00
			-0.1815E+00	0.0	0.3078E-03	0.8570E-05				
			-0.1815E+00	0.0	0.3078E-03	0.8570E-05				
			0.0	0.0	0.0	0.0				
			0.0	0.0	0.0	0.0				
			0.0	0.0	0.0	0.0				

RESPONSE NUMBER- 400 TIME SEGMENT- 2 TIME INCREMENT-320 GAMMA*DT= 0.1250E-03 DT= 0.1250E-01

STATE	TIME	ITER	STRESS	STRAIN	VP-STRAIN	VP-RATE	SJ1	SJ2	PHI	CAP EL
CAP - SS	5.000	1	-0.4202E+00	-0.3010E-01	-0.2671E-01	-0.2090E-06	-0.7835E+00	0.1877E-01	0.2956E-04	-0.7282E+00
			-0.1816E+00	0.0	0.3117E-03	0.7313E-07				
			-0.1816E+00	0.0	0.3117E-03	0.7313E-07				
			0.0	0.0	0.0	0.0				
			0.0	0.0	0.0	0.0				
			0.0	0.0	0.0	0.0				

RESPONSE NUMBER- 520 TIME SEGMENT- 3 TIME INCREMENT- 20 GAMMA*DT= 0.1250E-03 DT= 0.1250E-01

STATE	TIME	ITER	STRESS	STRAIN	VP-STRAIN	VP-RATE	SJ1	SJ2	PHI	CAP EL
ELASTIC	5.253	1	0.2980E+01	-0.2250E-01	-0.2671E-01	0.0	-0.3346E-01	0.1250E-02	0.0	-0.7282E+00
			-0.3163E+01	0.0	0.3117E-03	0.0				
			-0.3163E+01	0.0	0.3117E-03	0.0				
			0.0	0.0	0.0	0.0				
			0.0	0.0	0.0	0.0				
			0.0	0.0	0.0	0.0				

RESPONSE NUMBER- 560 TIME SEGMENT- 3 TIME INCREMENT- 40 GAMMA*DT= 0.1250E-03 DT= 0.1250E-01

STATE	TIME	ITER	STRESS	STRAIN	VP-STRAIN	VP-RATE	SJ1	SJ2	PHI	CAP EL
PSURF-VP	5.500	2	0.4079E+01	-0.2250E-01	-0.2603E-01	0.5573E-02	0.6268E+00	0.2969E-01	0.7850E+00	-0.7107E+00
			0.1094E+00	0.0	0.1993E-03	-0.8253E-03				
			0.1094E+00	0.0	0.1993E-03	-0.8253E-03				
			0.0	0.0	0.0	0.0				
			0.0	0.0	0.0	0.0				
			0.0	0.0	0.0	0.0				

RESPONSE NUMBER- 520 TIME SEGMENT- 5 TIME INCREMENT- 80 GAMMA*DT= 0.1250E-03 DT= 0.1250E-01

STATE	TIME	ITER	STRESS	STRAIN	VP-STRAIN	VP-RATE	SJ1	SJ2	PHI	CAP EL
PSURF-VP	6.500	1	0.1633E+01	-0.2250E-01	-0.2374E-01	0.6329E-03	0.3204E+00	0.2369E-02	0.6708E-01	-0.6531E+00
			0.7870E-01	0.0	-0.1827E-03	-0.1212E-03				
			0.7870E-01	0.0	-0.1827E-03	-0.1212E-03				
			0.0	0.0	0.0	0.0				
			0.0	0.0	0.0	0.0				
			0.0	0.0	0.0	0.0				

RESPONSE NUMBER- 600 TIME SEGMENT- 4 TIME INCREMENT-160 GAMMA*DT= 0.1250E-03 DT= 0.1250E-01

STATE	TIME	ITER	STRESS	STRAIN	VP-STRAIN	VP-RATE	SJ1	SJ2	PHI	CAP EL
PSURF-VP	7.500	1	0.1357E+00	-0.2250E-01	-0.2348E-01	0.7659E-04	0.2884E+00	0.1174E-02	0.1058E-01	-0.6472E+00
			0.7636E-01	0.0	-0.2334E-03	-0.1507E-04				
			0.7736E-01	0.0	-0.2334E-03	-0.1507E-04				
			0.0	0.0	0.0	0.0				
			0.0	0.0	0.0	0.0				
			0.0	0.0	0.0	0.0				

FOR SAMPLE OUTPUT OF VPDRVR UNIAXIAL STRAIN LOAD : MAX- GAMMA*DT= 0.1250E-03
MAX- DT= 0.1250E-01

NORMAL EXIT

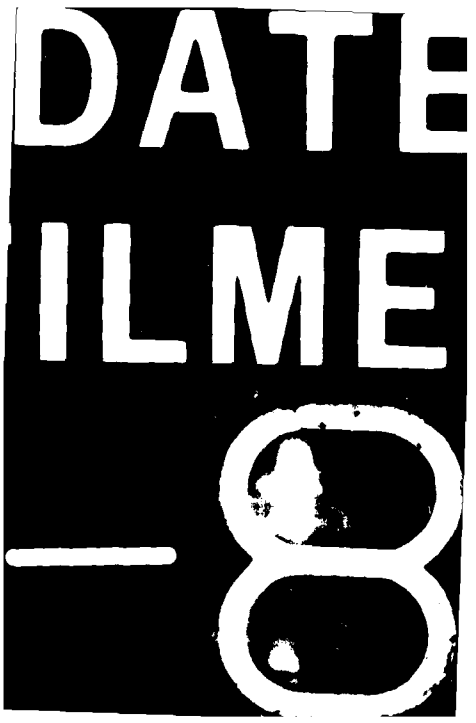
DATE:
ILME
8